

UCSF

UC San Francisco Previously Published Works

Title

Convergent neural representations of experimentally-induced acute pain in healthy volunteers: A large-scale fMRI meta-analysis.

Permalink

<https://escholarship.org/uc/item/25j6g4x2>

Authors

Xu, Anna

Larsen, Bart

Baller, Erica

et al.

Publication Date

2020-05-01

DOI

10.1016/j.neubiorev.2020.01.004

Peer reviewed



HHS Public Access

Author manuscript

Neurosci Biobehav Rev. Author manuscript; available in PMC 2020 December 22.

Published in final edited form as:

Neurosci Biobehav Rev. 2020 May ; 112: 300–323. doi:10.1016/j.neubiorev.2020.01.004.

Convergent neural representations of experimentally-induced acute pain in healthy volunteers: A large-scale fMRI meta-analysis

Anna Xu^a, Bart Larsen^a, Erica B. Baller^{a,b,c}, J. Cobb Scott^{a,d}, Vaishnavi Sharma^a, Azeez Adebimpe^a, Allan I. Basbaum^e, Robert H. Dworkin^f, Robert R. Edwards^g, Clifford J. Woolf^h, Simon B. Eickhoff^{i,j}, Claudia R. Eickhoff^{j,k}, Theodore D. Satterthwaite^{a,*}

^aDepartment of Psychiatry, University of Pennsylvania, Philadelphia PA 19104, USA

^bDepartment of Psychiatry, Massachusetts General Hospital, Boston, MA, USA

^cDepartment of Psychiatry, Harvard University, Boston, MA, USA

^dVISN4 Mental Illness Research, Education, and Clinical Center at the Philadelphia VA Medical Center, Philadelphia, PA, 19104, USA

^eDepartment of Anatomy, University of California, San Francisco, San Francisco, CA 94158, USA

^fDepartment of Anesthesiology and Perioperative Medicine, University of Rochester School of Medicine and Dentistry, Rochester, NY, USA

^gDepartment of Anesthesiology, Perioperative and Pain Medicine, Brigham and Women's Hospital, Harvard Medical School, Boston, MA, USA

^hFM Kirby Neurobiology Center, Boston Children's Hospital and Department of Neurobiology, Harvard Medical School, Boston, MA, USA

ⁱInstitute of Systems Neuroscience, Medical Faculty, Heinrich-Heine University, D-40225 Düsseldorf, Germany

^jInstitute of Neuroscience and Medicine, Brain & Behaviour (INM-1, INM-7), Research Centre Jülich, Germany

^kInstitute of Clinical Neuroscience and Medical Psychology, Medical Faculty, Heinrich-Heine-University, 40225 Düsseldorf, Germany

Abstract

Characterizing a reliable, pain-related neural signature is critical for translational applications. Many prior fMRI studies have examined acute nociceptive pain-related brain activation in healthy participants. However, synthesizing these data to identify convergent patterns of activation can be challenging due to the heterogeneity of experimental designs and samples. To address this

*Corresponding author at: Department of Psychiatry, University of Pennsylvania, 3400 Spruce St, Philadelphia, PA 19104, USA. sattertt@penmedicine.upenn.edu (T.D. Satterthwaite).

Appendix A. Supplementary data

Supplementary material related to this article can be found, in the online version, at doi:<https://doi.org/10.1016/j.neubiorev.2020.01.004>.

challenge, we conducted a comprehensive meta-analysis of fMRI studies of stimulus-induced pain in healthy participants. Following pre-registration, two independent reviewers evaluated 4,927 abstracts returned from a search of 8 databases, with 222 fMRI experiments meeting inclusion criteria. We analyzed these experiments using Activation Likelihood Estimation with rigorous type I error control (voxel height $p < 0.001$, cluster $p < 0.05$ FWE-corrected) and found a convergent, largely bilateral pattern of pain-related activation in the secondary somatosensory cortex, insula, midcingulate cortex, and thalamus. Notably, these regions were consistently recruited regardless of stimulation technique, location of induction, and participant sex. These findings suggest a highly-conserved core set of pain-related brain areas, encouraging applications as a biomarker for novel therapeutics targeting acute nociceptive pain.

Keywords

Pain; Neuroimaging; Meta-analysis; fMRI

1. Introduction

Chronic and acute pain are global medical issues affecting at least 20% of adults globally and they are often accompanied by both comorbid psychological disorders and significant disability in daily activities (Goldberg and McGee, 2011). Given the prevalence of pain conditions, there is a need to develop tools capable of translating the subjective report of pain into an objective measure (i.e., a pain biomarker) that can be used in the development of novel treatments. Recently, neuroimaging approaches have been used to examine pain-related brain activity as a physiological biomarker of pain for treatment development (Cowen et al., 2015; Labus et al., 2015; Wager et al., 2013; Woo et al., 2017). Though the challenge of pain biomarker development is increased when chronic pain conditions are analyzed, a growing body of work examining the neural correlates of experimentally-induced, nociceptive pain in healthy volunteers has led to important insights into the mechanisms and characteristics of how the sensation of pain arises, including its cognitive, affective, and sensory dimensions that may not be reflected in self-report scales (Apkarian et al., 2005; Hofbauer et al., 2001; Robinson et al., 2013; Talbot et al., 1991; Tracey and Mantyh, 2007; Treede et al., 1999; Woo and Wager, 2016). While this work has been critical in elucidating the circuits recruited by acute nociceptive pain under a variety of experimental contexts, synthesizing these data to identify convergent patterns of pain-related brain activation can be challenging due to heterogeneity of experimental designs and samples.

To integrate findings across neuroimaging experiments, meta-analysis provides a powerful approach to quantitatively identify consistent brain regions activated during pain (Wager et al., 2009). Prior meta-analyses have identified several brain regions that are engaged under pain conditions, including the secondary somatosensory cortex (SII), insula, cingulate cortex, and thalamus. Other regions have been identified somewhat less reliably, including primary somatosensory cortex (SI), striatum, cerebellum, supplementary motor area (SMA), primary motor area (M1), periaqueductal gray (PAG), prefrontal cortex (PFC), certain areas in parietal cortices, and the parahippocampal gyrus (Apkarian et al., 2005; Duerden and Albanese, 2013; Farrell et al., 2005; Jensen et al., 2016; Lanz et al., 2011; Peyron et al.,

2000; Tanasescu et al., 2016). Subsequent meta-analyses have sought to parse this pain network further by investigating neural responses specific to different pain induction modalities, such as thermal pain (Farrell et al., 2005; Friebe et al., 2011; Jensen et al., 2016), and to different stimulation location (Duerden and Albanese, 2013; Jensen et al., 2016; Lanz et al., 2011). These meta-analyses have provided a substantial advance in our understanding of the brain's pain network. However, the significant increase in functional magnetic resonance imaging (fMRI) experiments in pain since the most recent meta-analyses (Jensen et al., 2016; Tanasescu et al., 2016) as well as an influx of articles standardizing rigorous procedures for meta-analyses (Eickhoff et al., 2016; Müller et al., 2018) suggest that an update is warranted. Furthermore, based on recent evidence of inadequate Type I error control using previously-typical statistical methods, we considered it worthwhile to revisit the topic of identifying brain regions consistently recruited by diverse pain-inducing stimuli while adhering to contemporary standards in the field (Eklund et al., 2016; Müller et al., 2018).

Accordingly, we conducted a comprehensive meta-analysis of fMRI studies of experimentally-induced pain in healthy volunteers; the analysis included findings from 222 experiments. We first sought to replicate and extend the findings from previous meta-analyses, incorporating more recent studies in this rapidly moving field. Second, we applied standards for Type I error correction to our analyses according to current standards in the field. Third, we assessed differences in pain responsiveness associated with differences in pain stimulation modality (thermal, electrical, mechanical, or chemical), location of stimulation (visceral or somatic, left or right side of body, proximal or distal extremity), and sample composition (participant sex). As described below, our results revealed highly convergent evidence for the existence of a core set of brain regions associated with acute nociceptive pain in healthy participants. This core set was present across different samples and experimental designs, encouraging its use as biomarker of acute pain that could be useful for experimental therapeutics.

2. Methods

This is a systematic review and meta-analysis, and the methodology used adheres to PRISMA and field-standard guidelines for meta-analyses (Moher et al., 2009; Müller et al., 2018). The procedures and analyses in this meta-analysis were preregistered on PROSPERO (https://www.crd.york.ac.uk/prospERO/display_record.php?RecordID=106435).

We first performed a literature search for fMRI experiments of experimentally induced pain in healthy participants using eight databases and then searched for references in reviews identified in the database. Titles and abstracts returned by this search were first evaluated for full-text screening. Full text articles were evaluated to see if they met defined inclusion criteria (see Fig. 1 for PRISMA chart detailing screening process). This screening process resulted in a total of 222 fMRI experiments from 200 articles that were included in this study. See specific details below. Coordinate data from these experiments were then extracted and analyzed using activation likelihood estimation (ALE).

2.1. Literature search

We performed a literature search for fMRI experiments of experimentally induced pain in healthy volunteers using both database searches and references cited in review articles, meta-analyses, and component studies. The final literature search took place on August 1, 2018 and was restricted to articles published from 1990 to August 1, 2018. We used 1990 as the start date of our search due to the widespread emergence of using fMRI for neuroimaging tasks such as pain starting after 1990.

2.1.1. Database search—The following standard literature databases were searched: PUBMED/MEDLINE, EMBASE, Web of Science, Cochrane Library, and PsycINFO. We used the following search terms: (“MRI” or “magnetic resonance imaging” or “fMRI” or “BOLD” or “brain mapping”) AND (“pain” or “noxious” or “nociception”). We further filtered our search criteria to try to meet our inclusion criteria (section 2.2) by including only publications that were in English, that appeared in peer-reviewed journals (e.g., not conference papers), and that included experiments conducted in humans. We supplemented our database search with the following existing fMRI data repositories: NeuroSynth (Yarkoni et al., 2011), brainspell (Toro, 2015), and BrainMap (Laird et al., 2005). In these repositories, we searched for records using the keyword “pain.” Notably, we did not include grey literature in our search, as this could introduce studies that did not undergo peer review, potentially compromising the rigor of our methodology.

2.1.2. Reference search from reviews—To identify potential candidate studies from reference lists, we also screened the resulting abstracts for editorials, review articles, and meta-analyses related to pain. In editorials (i.e., non-systematic reviews), we identified titles in reference sections that seemed likely to include a pain experiment. In systematic reviews, we considered all articles that the authors identified for inclusion. If a systematic review included a meta-analysis of experimentally induced pain in healthy volunteers (e.g., Friebel et al., 2011; Duerden and Albanese, 2013; Jensen et al., 2016; Tanasescu et al., 2016), we automatically included all studies within the meta-analysis to be screened for full text.

The database search yielded a total of 7,529 articles. We additionally compiled references from existing review articles which yielded a total of 1,216 articles (total of 8,754 records). After removing duplicates, we screened a total of 4,927 abstracts.

2.2. Screening

2.2.1. Inclusion criteria—Experiments were only included in the meta-analysis if they contained a within-subject “pain > baseline” contrast (e.g., “pain > rest”, “pain > innocuous stimuli” or parametric modulation of pain) that was not confounded by other experimental manipulations that could impact the acute nociceptive pain induction (e.g., treatment manipulations prior to the pain induction, such as drug infusions or placebo). If at least one experiment in an article satisfied this initial requirement, it was evaluated according to the following inclusion criteria:

1. The experiment was from a peer-reviewed journal article written in English. Prior literature has shown language restrictions to English have marginal effect on results and are dependent on the field of study (Morrison et al., 2012). We

therefore did not feel this language restriction would introduce substantial bias to our results.

2. The experiment considered healthy, human participants aged 18 or over. To satisfy this criterion, the study must explicitly report that all participants were healthy or free of medical or psychiatric disorders.
3. The experiment included at least 10 participants.
4. The experiment induced physical pain that was confirmed to be painful by participants. Confirmation of experienced pain could be in the form of an explicit report of the induction being painful, participant ratings of experienced pain during the scan session, or the use of a pain stimulus that was titrated to a threshold pre-determined to be painful by participants in the experiment.
5. Brain responses to induced pain were monitored using fMRI.
6. The field of view and reported results included the whole brain (i.e., region of interest analyses were excluded). This criterion was imposed so as to prevent bias towards *a priori* regions putatively thought to be involved in pain.
7. The experiment reported results in a standard stereotaxic reference space coordinate system (MNI or Talairach space).
8. Results met current statistical standards for conventional cluster identification. Specifically, we only included experiments that reported activation at a voxel-level threshold of $p < 0.001$ (uncorrected) or a corrected cluster probability of $p < 0.05$. We also excluded experiments that did not report their methods and results in sufficient detail to conclude whether they met our statistical threshold criteria.

Additionally, if experiments in articles did not report relevant results but met the inclusion criteria, we e-mailed the corresponding authors and included the experiment if data was provided. A PICOS figure of our search and eligibility criteria is included in Supplementary Table 2.

2.2.2. Abstract and full text assessment—Two independent reviewers (AX, EBB) confirmed the inclusion or exclusion of each abstract for full text screening. Abstracts were first assessed as to whether they included a physical pain contrast in healthy volunteers and whether they measured task-based blood-oxygen-level-dependent (BOLD) responses. In this stage of screening, we only excluded abstracts that explicitly mentioned (1) having a sample size of less than 10 subjects; (2) using only a neuroimaging modality that was not fMRI, such as EEG; or (3) only including animal experiments. Note that in this stage of screening, we did not exclude any papers that involved a clinical population, used resting-state fMRI, or involved a treatment or intervention. These criteria allowed us to assess parts of seemingly irrelevant papers that may have included relevant experiments for analyses, such as including a healthy subsample (e.g., the control sample) or a task-based measure involving acute nociceptive pain (e.g., pain inductions either pre-treatment or post-resting-state). Full text articles from included abstracts were then assessed for whether they met our inclusion criteria (see section 2.2.1. Inclusion Criteria). Finally, at least two independent

reviewers confirmed the decision for inclusion of articles marked for inclusion in the final analysis (AX, BL, EB). In cases of reviewer decision disagreement, a senior third reviewer (TS) evaluated the article.

2.3. Data extraction

Coordinates and information about each experiment were extracted manually by at least one author (AX or VS) and checked independently by another member of the study team (AX or VS). The following information about each paper was extracted: sample size; whether the coordinate space was MNI or Talairach; modality of pain stimulus (e.g., thermal, electrical, mechanical, or chemical); side the stimulus was induced; whether the stimulus was on the arm (not including hand), leg (not including foot), hand, or foot; whether the pain stimulus was visceral (e.g., esophageal distension); and whether the reported activation included a non-painful control stimulus (e.g. painful > innocuous contrast).

In cases where studies contained multiple relevant pain contrast results from a single experiment, we chose to use results that were most likely to demonstrate a clear nociceptive pain-specific signal. For example, when experiments contained separate analyses based on the intensity of the pain induction (e.g., one contrast for moderate pain and another for high pain), we chose the contrast for the highest intensity of pain reported (e.g., high pain). For experiments with separate analyses based on a subjective rating of pain and based on an objective intensity, we included results based on the objective intensity rather than the subjective rating.

If multiple experimental contrasts included in a single article could be used for different sets of meta-analyses (see section 2.4.2.), we first pooled coordinates from each experiment into one set of coordinates for that particular article and treated this set of coordinates as one experiment in our primary meta-analysis (Turkeltaub et al., 2012). This approach ensured that we only used one set of coordinates per article, so that one specific article could not be weighted more heavily than others due to the presence of multiple relevant experiments (Müller et al., 2018; Turkeltaub et al., 2012). For example, for our primary meta-analysis of experimentally-induced pain, if an article contained multiple experiments using different types of pain stimulation (e.g., thermal and mechanical), we pooled the results from both types of pain stimulation together and treated the results as if they were derived from one experiment. For any additional analyses (see section 2.4.2.), we evaluated these contrasts separately (e.g., the thermal set of coordinates would be tagged as thermal pain and treated as one experiment while the mechanical set of coordinates would be tagged as mechanical pain and treated as another experiment).

2.4. Coordinate based meta-analysis

2.4.1. Activation likelihood estimation (ALE)—We conducted meta-analyses using the coordinate-based meta-analytic method activation likelihood estimation (ALE) (Turkeltaub et al., 2002) using the revised algorithm that allows for random effects inference (Eickhoff et al., 2009, 2012; Rottschy et al., 2012). The main effect for a particular condition of interest is defined by the convergence of activation from all relevant experiments included in analyses.

Briefly, for each experiment included, ALE treats coordinates for the foci of reported clusters as the center of an uncertainty function modeled by a 3D Gaussian probability distribution. The full width at half-maximum (FWHM) of this 3D Gaussian kernel was determined by empirical data on between-subject and between-template (i.e., MNI or Talairach space coordinates) variance. Specifically, the algorithm takes into account between-subject variance by using a tighter Gaussian distribution for experiments with greater sample sizes to represent that these experiments should provide more reliable results of a true activation effect (Eickhoff et al., 2009), and it takes into account between-template differences by transforming coordinates reported in Talairach coordinates into MNI coordinates (Lancaster et al., 2007). This model then provides probabilities for all activation foci in each experiment, which were combined for each voxel, resulting in an individual modeled activation (MA) map for each experiment. By taking the union across all the MA-maps, we generated voxelwise ALE scores that describe the convergence of results at each particular location (Eickhoff et al., 2009). Note that MA-values reflect data for a single experiment while ALE-values integrate data across multiple experiments.

For ALE maps, the p -value was defined as the proportion of values obtained under a null distribution reflecting a random spatial association between experiments. The resulting non-parametric p values were subsequently thresholded using voxel height threshold of $p < 0.001$, reflecting current recommendations for best practices (Eklund et al., 2016). At this voxel height, the significance of cluster extent was estimated using 10,000 Monte-Carlo simulations; this distribution was calculated specifically for each meta-analysis conducted (Eickhoff et al., 2012; Rottschy et al., 2012). Clusters were considered significant if they achieved a family-wise corrected significance of $p < 0.05$. Prior to display, p -values were then transformed into z scores. All results were labeled using either SPM Anatomy Toolbox v2.2 (Eickhoff et al., 2005) or Harvard-Oxford Structural Atlas (Kennedy et al., 1998) distributed by FSL. Thalamic parcellations included with SPM Anatomy Toolbox were based on the Thalamic Connectivity Atlas (Behrens et al., 2003).

2.4.1.1. *Statistical contrasts.* To analyze differences in convergent activation (i.e., differing convergence of results) between two different groups of experiments, we computed the voxel-wise differences between the cluster-level FWE-corrected maps derived from the individual main effect analyses (as described above). To determine the significant difference in ALE scores, we first generated a null distribution of ALE-score differences by randomly permuting the labels of all experiments, dividing them into two groups of the same sizes as the original analysis, and calculating the ALE-scores for these two randomly permuted groups for all voxels in the brain. We repeated this process 10,000 times and tested the observed differences in ALE-scores against the derived null distribution. We thresholded probability values at $p < 0.001$ and inclusively masked them by the main effects for the particular condition of interest. Finally, we applied an extent-threshold of $k > 25$ voxels. It is important to note, however, that an unequal proportion of experiments in the two groups of interest could bias the observed results. To address this concern, we conducted chi-squared tests for differences in proportion of experiments between the two groups of interest in each of our planned contrasts, and we limited our analyses to comparisons that did not significantly differ in number of experiments (at $p < 0.01$).

2.4.1.2. Conjunction analyses.: To analyze voxels where a significant effect was present in two different groups of experiments, we computed their conjunction using the conservative minimum statistic (Nichols et al., 2005). This approach is equivalent to identifying the intersection between each of the cluster-level FWE-corrected maps of the main effects for the two groups of experiments (Caspers et al., 2010). We then applied an extent-threshold of $k > 25$ voxels to exclude smaller regions of presumably incidental overlap between the two maps of the main effects.

2.4.2. Effects of interest—We primarily focused on finding areas consistently reported to be activated in response to noxious stimuli inducing acute pain. We first assessed areas converging in activation in response to pain using all of our extracted coordinate data (with only one set of coordinates per article). However, because some of our included experiments used a contrast of “pain > rest” while others used a contrast of “pain > innocuous stimuli”, we conducted secondary analyses examining the main effect of the experiments using the contrast “pain > rest” and then the experiments using “pain > innocuous stimuli.” A contrast between experiments using “pain > rest” contrast and “pain > innocuous stimuli” contrast, however, was not computed due to significant differences in the proportion of experiments using the “pain > rest” contrast and the “pain > innocuous stimuli” contrast.

Next, given the heterogeneity of the different pain induction techniques used in the included experiments, we conducted additional contrast and conjunction analyses that examined the effect of different modalities and locations of pain inductions as well as the sex of the sample. The following analyses were conducted:

- To analyze the effect of pain modalities considered, we examined experiments inducing thermal pain (e.g., heat, cold), mechanical pain (e.g., pin prick, pressure, distension), electrical pain (e.g., electrical stimulation), and chemical pain (e.g., capsaicin). To explicitly compare different modalities, we conducted between-experiment contrasts comparing thermal and non-thermal experiments as well as electrical and mechanical experiments. Further analyses comparing other modalities could not be reliably conducted based on significant differences in the proportion of experiments available.
- To examine effects of the location of induced pain, we conducted three separate contrasts. First, we evaluated laterality by contrasting experiments where pain was induced on the left side versus the right side of the body. Second, we examined differences in the effect of inducing pain on the extremities at proximal (i.e., the arm or leg) versus distal (i.e., the hand or foot) locations, which have different densities of nociceptors. Third, we examined differences in brain activation for visceral (e.g., rectal distension) versus non-visceral (i.e., somatic) pain. Notably, we only included non-visceral mechanical pain, because all visceral pain inductions were mechanical.
- Finally, by comparing experiments that included *only* male or *only* female participants, we sought to evaluate sex differences in the pain response.

2.4.3. Post-hoc diagnostics—To address bias and heterogeneity of experiments included in our primary meta-analysis of pain, we calculated the contribution of each experiment by computing the ratio of ALE-scores of all voxels in a specific cluster with and without each experiment. Similarly, we calculated the contribution of different conditions of interest from groups of experiments (e.g., thermal, mechanical, right-sided pain, left-sided pain, etc.). These analyses provided an estimate of how the ALE-score changed when the experiment or group of experiments in question was removed (see Cieslik et al., 2016 for example). However, given the large number of experiments included in this study, undue influence of a single experiment was relatively unlikely (Eickhoff et al., 2012).

3. Results

Our search, screening, and evaluation yielded a total of 222 experiments from 200 articles that met inclusion criteria as confirmed by two independent reviewers (Fig. 1). Of these 222 experiments, we meta-analyzed 200 experiments for the main effect of induction of a reported sensation of pain. Among these, 62 experiments used a “pain > innocuous” contrast and 134 experiments used a “pain > rest” contrast. The remaining 3 experiments examined a parametric modulation of pain.

For modality-specific analyses, we meta-analyzed 107 thermal pain experiments (inducing heat pain or cold pain) and 98 non-thermal pain experiments. The non-thermal pain experiments included 39 experiments inducing electrical pain (e.g., electric shocks), 46 inducing mechanical pain (e.g., pressure pain, distension), and 13 inducing chemical pain (e.g., capsaicin). For location-specific analyses, we meta-analyzed 92 left-sided pain experiments, 66 right-sided pain experiments, 68 experiments inducing pain in distal extremities, 85 experiments inducing pain in proximal extremities, 17 experiments inducing visceral pain, and 29 experiments inducing non-visceral (mechanical) pain. Finally, for sample composition-related analyses, we meta-analyzed 22 all-female experiments and 30 all-male experiments (Fig. 2; Table 1).

3.1. Main effect of stimuli inducing a sensation of pain

Meta-analysis of pain experiments from all studies ($n = 200$), which included experiments using the contrasts “pain > rest” and “pain > innocuous” as well as parametric modulation of pain, revealed significant pain-related convergence of activation in four large clusters, with peak activation magnitudes located in the right supramarginal gyrus (inferior parietal lobule, IPL), right midcingulate cortex (MCC), right precentral gyrus, and left cerebellum (Fig. 3; Table 2). Further examination of these large clusters revealed activation in the bilateral thalamus, bilateral SMA, bilateral pre-SMA, bilateral putamen, bilateral caudate, bilateral brainstem, bilateral amygdala, right middle frontal gyrus, left supramarginal gyrus/IPL (insula) and left MCC. Post-hoc analysis confirmed these results were not significantly impacted by any individual experiment (see Supplementary Table 1).

We next evaluated experiments reporting a “pain > rest” contrast ($n = 134$) and “pain > innocuous” contrast ($n = 62$), as “pain > innocuous” contrasts controlled for the impact of sensorimotor stimulation (e.g., touch). In experiments reporting a “pain > rest” contrast, we found significant activation in seven clusters, with peak activation magnitudes located in

bilateral IPL (right supramarginal gyrus and left intraparietal sulcus), right MCC, right precentral gyrus, left insula, left thalamus, and left cerebellum (Fig. 4A; Table 3). Activation in these clusters also comprised of bilateral SMA, bilateral pre-SMA, bilateral putamen, bilateral caudate, right brainstem, right insula, right middle frontal gyrus, right amygdala, left MCC, and left precentral gyrus. In experiments using a “pain > innocuous” contrast, we found significant activation in four clusters, with peak activation magnitudes located in bilateral insula, right MCC, and right thalamus (Fig. 4B; Table 3). These clusters were also comprised of the bilateral putamen, bilateral SMA, left MCC, left thalamus, right amygdala, right precentral gyrus and right pre-SMA. Due to statistically significant differences in number of experiments reporting these contrasts ($\chi^2(1) = 27.33, p < 0.001$), we did not perform an explicit contrast between experiments reporting a “pain > rest” contrast and a “pain > innocuous” contrast.

3.2. Effect of stimulus modality

3.2.1. Thermal and non-thermal pain—To examine modality-specific effects of pain induction, we first compared experiments that induced thermal pain ($n = 107$) with experiments that induced non-thermal pain ($n = 98$). Experiments inducing thermal pain showed convergence of activation in five clusters, with peak activation magnitudes located in right Rolandic operculum/IPL (posterior insula), right MCC, right middle frontal gyrus, right precentral gyrus, and left cerebellum (Fig. 5A; Table 4). Further examination of these large clusters revealed activation in bilateral putamen, bilateral caudate, bilateral brainstem, bilateral SMA, bilateral pre-SMA, left Rolandic operculum/IPL, left MCC, and right amygdala. Experiments inducing non-thermal pain also showed activation in five clusters, with peak activation magnitudes located in right Rolandic operculum, right MCC, right thalamus, right middle frontal gyrus, and left postcentral gyrus (SII) (Fig. 5B; Table 4). Further examination of these large clusters revealed activation in bilateral SMA, bilateral putamen, bilateral pre-SMA, left MCC, and left thalamus. An explicit contrast between thermal and non-thermal pain experiments revealed significantly stronger convergence of activation in bilateral MCC for thermal experiments, and stronger convergence in the right insula and left Rolandic operculum in non-thermal experiments (Table 4). Conjunction analyses revealed widespread overlap between thermal and non-thermal pain experiments in six large clusters, with peak activation magnitudes located in bilateral supramarginal gyrus (SII), bilateral thalamus, right MCC, and right middle frontal gyrus (Table 4). These large clusters also included the bilateral putamen, bilateral SMA, left MCC, and right amygdala.

3.2.2. Electrical, mechanical, and chemical pain—We next examined the effect of electrical ($n = 39$), mechanical ($n = 46$), and chemical ($n = 13$) pain induction (Figs. 6 and 7). Experiments inducing electrical stimulation to evoke pain showed convergence of activation in five large clusters, with peak activation magnitudes located in bilateral thalamus, right MCC, right Rolandic operculum, and left postcentral gyrus (SII) (Fig. 6A; Table 5). Experiments inducing mechanical pain showed convergence of activation in seven large clusters, with peak activation magnitudes located in bilateral insula, bilateral supramarginal gyrus (consisting of SII and IPL), bilateral thalamus, and right MCC (Fig. 6B; Table 5). Further examination of these large clusters associated with mechanical pain revealed activation including the bilateral putamen and left MCC. An explicit contrast

between electrical and mechanical pain experiments revealed greater activation in the right Rolandic operculum, right thalamus, and right superior temporal gyrus in electrical pain experiments. In no cases was greater activation seen for mechanical pain experiments (Table 5). Conjunction analyses revealed widespread overlap of convergence of activation between electrical and mechanical pain experiments in seven large clusters, with peak activation magnitudes located in bilateral insula, bilateral SII (left postcentral gyrus and right supramarginal gyrus), bilateral thalamus, and right MCC (Table 5).

Finally, chemical pain experiments showed convergence of activation in ten clusters, with peak activation magnitudes located in ventral aspects of the brainstem, bilateral insula (with two clusters in the left insula), bilateral thalamus, left Rolandic operculum, left MCC, left SMA, and right postcentral gyrus/IPL (Fig. 7; Table 6). Further examination of these large clusters revealed activation within the right MCC and midbrain. There were not a sufficient number of chemical pain induction comparisons to contrast chemical pain-related activation with electrical stimulation-provoked pain ($X^2(1) = 13, p < 0.001$), mechanical pain ($X^2(1) = 18.45, p < 0.001$), or thermal pain ($X^2(1) = 73.63, p < 0.001$).

3.3. Effect of stimulus location

3.3.1. Laterality—To examine location-specific effects of nociceptive pain induction, we compared experiments that induced left-sided pain ($n = 92$) with experiments that induced right-sided pain ($n = 66$). Experiments inducing left-sided pain showed convergence of activation in six clusters, with peak activation magnitudes located in right Rolandic operculum, right MCC, right middle frontal gyrus, and right postcentral gyrus, left supramarginal gyrus, and left cerebellum (Fig. 8A; Table 7). Further examination of these large clusters revealed activation in bilateral insula, bilateral thalamus, bilateral pre-SMA, left MCC, right amygdala, right pallidum and the brainstem. Experiments inducing right-sided pain showed convergence of activation in nine clusters, with peak activation magnitudes located in bilateral thalamus, left Rolandic operculum, right supramarginal gyrus, right MCC, right middle frontal gyrus, right IPL, right precentral gyrus and right insula (Fig. 8B, Table 7). Further examination of these large clusters revealed activation in bilateral putamen, bilateral SMA, bilateral pre-SMA, left MCC, left insula, and right precentral gyrus.

An explicit contrast between left- and right-sided stimulation experiments did not reveal any clusters with stronger convergence of activation in left-sided pain induction experiments but did reveal stronger convergence of activation in left Rolandic operculum (SII) in right-sided pain induction experiments (Table 7). Given that we did not see involvement of SI in right-sided pain induction based on these analyses (despite reports of SI involvement in pain (Bushnell et al., 1999), we also separately examined unthresholded maps and found involvement of right SI, suggesting that while SI did not appear prominently in our explicit contrast, there may still be some laterality in SI that is harder to detect. SI was particularly prominent when the stimulation site was more tightly aligned across studies (e.g., left-sided arm stimulation).

Finally, conjunction analyses revealed widespread overlap of convergence of activation between left-sided and right-sided experiments in eight clusters, with peak activation

magnitudes located in bilateral insula, bilateral supramarginal gyrus (consisting of IPL), bilateral thalamus, right MCC, and right middle frontal gyrus (Table 7). Further evaluation of these clusters revealed activation in the left MCC, right putamen, and right SMA.

3.3.2. Distal and proximal extremities—We next compared experiments inducing distal nociceptive pain in the hand or foot ($n = 68$) with experiments inducing proximal pain in the arm or leg ($n = 85$). Experiments inducing distal pain in the hand or foot also showed convergence of activation in six clusters, with peak activation magnitudes located in bilateral IPL (consisting of right Rolandic operculum and left supramarginal gyrus), bilateral thalamus, right MCC, and right middle frontal gyrus (Fig. 9A; Table 8). Further examination of these large clusters revealed activation in bilateral insula, bilateral amygdala, bilateral pre-SMA, and right SMA. Experiments inducing proximal pain showed convergence of activation in six clusters, with peak activation magnitudes located in right Rolandic operculum, right MCC, right middle frontal gyrus, right precentral gyrus, right post central gyrus, and left insula (Fig. 9B; Table 8). These large clusters included the bilateral pre-SMA, bilateral subnuclei of the striatum, right insula, right SMA, and left MCC. An explicit contrast between proximal and distal stimulation experiments did not reveal differential patterns of activation, while conjunction analyses revealed widespread overlap convergence of activation in eight clusters (Table 8). These eight clusters included bilateral thalamus, bilateral IPL (represented by left supramarginal gyrus and right operculum), right MCC (with spread to left MCC), right middle frontal gyrus, right pallidum, and left insula.

3.3.3. Effect of acute visceral and non-visceral mechanical nociceptive pain—We compared experiments inducing visceral pain (e.g., distension in the rectum, esophagus, or stomach; $n = 17$) with experiments inducing non-visceral mechanical pain ($n = 29$). Experiments inducing visceral pain showed convergence of activation in five clusters, with peak activation magnitudes located in right supramarginal gyrus, right Rolandic operculum, left putamen, left thalamus, and right MCC (Fig. 10A; Table 9). Non-visceral mechanical pain experiments showed convergence of activation in ten clusters, with peak activation magnitudes located in bilateral supramarginal gyrus (SII), bilateral insula (with two clusters in the right insula), bilateral thalamus, right Rolandic operculum, right caudate nucleus, and right MCC (Fig. 10B; Table 9). An explicit contrast between visceral and non-visceral mechanical pain experiments did not reveal differential activation, while conjunction analyses revealed overlap of convergence in two clusters—the right supramarginal gyrus and the left thalamus (Table 9).

3.4. Effect of sex

We examined sex differences in nociceptive pain responses by comparing experiments with an all-female sample ($n = 22$) to those with an all-male sample ($n = 30$). Experiments with an all-female sample showed convergence of activation in five clusters, with peak activation magnitudes located in bilateral IPL (represented by left superior temporal gyrus and right supramarginal gyrus) and bilateral insula (with two clusters in the left insula; see Fig. 11A and Table 10). Experiments with an all-male sample showed convergence of activation in eight clusters, with peak activation magnitudes located in bilateral insula, bilateral thalamus, right MCC (spreading into the left hemisphere), right temporal pole (spreading into the

precentral gyrus), right middle frontal gyrus and right Rolandic operculum (Fig. 11B; Table 10). An explicit contrast between males and females did not reveal differential activation (Table 10), while conjunction analyses revealed overlap in three clusters—bilateral insula and left supramarginal gyrus/IPL (Table 10).

4. Discussion

We conducted what is to our knowledge the largest fMRI meta-analysis of experimentally induced pain in healthy volunteers to date, applying rigorous type I error control and stringent inclusion criteria. We first synthesized results across 200 experiments, revealing a network of regions consistently activated by acute nociceptive pain in healthy participants. We further interrogated the modulation of stimulation modality, stimulation location, and sex and found a largely consistent pattern of activation in a core set of brain regions, irrespective of the specific experimental paradigm. These regions include the thalamus, MCC, SII, insula, as well as portions of the supramarginal gyrus/IPL and Rolandic operculum. In a smaller number of analyses, we observed involvement of the lateral PFC, precentral gyrus, SMA, pre-SMA, cerebellum, the brainstem, basal ganglia (putamen, caudate, and palladium), amygdala, and postcentral gyrus (SI; Fig. 12).

Our primary meta-analysis revealed a “pain network” of convergent activation across 200 experiments that was largely consistent with the findings of other similar recent meta-analyses (Friebel et al., 2011; Duerden and Albanese, 2013; Jensen et al., 2016; Tanasescu et al., 2016). As in prior meta-analyses, we found evidence of pain-related activation of bilateral thalamus, cingulate cortex, insula, SII, motor areas, and right middle frontal gyrus (Friebel et al., 2011; Duerden and Albanese, 2013; Jensen et al., 2016; Tanasescu et al., 2016). However, a subset of brain areas identified here are less consistently reported in earlier work, including the basal ganglia (putamen) (Duerden and Albanese, 2013; Jensen et al., 2016; Tanasescu et al., 2016), the amygdala (Jensen et al., 2016; Tanasescu et al., 2016), and the brainstem (Tanasescu et al., 2016). Notably, previous meta-analyses have reported activation in SI and the right cerebellum (Duerden and Albanese, 2013; Jensen et al., 2016; Tanasescu et al., 2016), which were not found here. To the degree that there is variation between our results and prior meta-analyses, these may in part reflect differences in the sample and methodological approach. Specifically, we considered the largest sample to date of studies which passed rigorous inclusion criteria (e.g., at least 10 participants, cluster $p < 0.001$ or FWE-corrected). Additionally, in line with current recommendations (e.g., Eklund et al., 2016 and Eickhoff et al., 2016), we applied a more stringent statistical correction to our results than prior meta-analyses.

We found qualitative evidence for more activation of SII, insula, MCC, thalamus, SMA, pre-SMA, MCC, and right amygdala in experiments using an innocuous control compared to those that used a resting baseline. In contrast, experiments using a resting baseline had significant convergence of activation in right lateral PFC, right precentral gyrus, left cerebellum, and bilateral subnuclei of the basal ganglia (putamen, caudate) that were not identified in our analysis of experiments using an innocuous control. These findings suggest that these areas may not be response to pain per se, but rather a general response to sensory stimulation. While these qualitative findings are interesting, we did not conduct a direct,

quantitative comparison of studies using a sensorimotor control and a resting baseline due to differences in the number of experiments using these approaches. Specifically, there was a significantly greater number of experiments using a resting baseline than experiments using an innocuous control. As such, it is difficult to conclude whether observed differences are in part driven by differences in the number of experiments included. Nevertheless, the qualitative differences between these two contrasts may still be meaningful and ultimately expected, as contrasts against a resting baseline will also reflect sensorimotor processing. To better separate the pain response from non-specific sensory responses, studies are needed that explicitly compare these two baseline conditions.

To further interrogate variability in the pain response that may be sensitive to differences in other experimental design considerations, we conducted a set of sub-analyses that investigate the effects of stimulation modality, stimulation location, and sex of sample. These analyses revealed a core set of brain areas that were consistently and robustly activated by pain regardless of experimental design, as well as regions that are more variably activated by pain across experiments. We discuss these areas in detail below.

4.1. Core regions consistently activated by pain

The thalamus, SII, MCC, and insula were the most robustly activated brain areas across all experimental paradigms. This core set of brain regions has been implicated in sensory-discriminative and affective-motivational aspects of pain (Tracey and Mantyh, 2007; Treede et al., 1999). The thalamus processes and transmits nociceptive information between the spinal cord and cortex (Yen and Lu, 2013; Ab Aziz and Ahmad, 2006) while the SII may reflect higher-order sensory representation, especially information from sensory stimuli requiring more attention (Chen et al., 2008; Ferretti et al., 2003). Here, we found consistent activation of SII even in experiments that include a specific sensorimotor control condition, supporting a role for SII that goes beyond basic sensory processing, and concords with previous pain imaging studies demonstrating bilateral SII activation (Mazzola et al., 2006).

The MCC is strongly implicated in the affective-motivational components of pain, especially pain response selection (Medford and Critchley, 2010; Shackman et al., 2011; Vogt, 2005, 2016; Vogt et al., 2003), and has been reported in previous meta-analyses of pain (Farrell et al., 2005; Friebel et al., 2011; Peyron et al., 2000; Tillisch et al., 2011). While other meta-analyses and reviews have highlighted involvement of the anterior cingulate (ACC) in pain (Apkarian et al., 2005; Duerden and Albanese, 2013; Jensen et al., 2016; Lanz et al., 2011; Peyron et al., 2000), it should be noted that our MCC results overlap with what has sometimes been labeled as ACC. Moreover, the convergence of mid-cingulate activation associated with pain (rather than anterior regions of the cingulate) support delineations of the cingulate cortex, with the middle cingulate being more involved in pain compared to anterior regions (Shackman et al., 2011; Vogt, 2016).

The insula is thought to play a more indirect role in pain perception by integrating exteroceptive and interoceptive information into awareness and subjective feelings towards salient information (Craig et al., 2000; Isnard et al., 2011; Craig, 2009; Kurth et al., 2010), especially via its functional connections to the cingulate cortex (Taylor et al., 2009). The posterior portion of the insula in particular has been implicated in processing bodily

information (e.g., painful sensations, somatosensory stimulation, interoception) while the anterior insula may be more involved in salience detection (Craig, 2009; Kurth et al., 2010; Menon and Uddin, 2010). As such, our meta-analytic findings of widespread insula activation associated with pain are consistent with involvement of both anterior and posterior insula involved in acute nociceptive pain (Kurth et al., 2010).

4.2. Regions less consistently activated by pain

In addition to the core set of pain-sensitive brain areas described above, a broader set of pain-associated regions were somewhat less consistently recruited, emerging only in specific cases. These regions include the lateral PFC, M1, SMA (and portions of the pre-SMA), cerebellum, brainstem, SI, basal ganglia (putamen, caudate, and pallidum), and the amygdala. These areas have been previously reported to have less consistent and possibly more nuanced involvement in responses to pain (Apkarian et al., 2005; Duerden and Albanese, 2013; Farrell et al., 2005; Friebel et al., 2011; Lanz et al., 2011; Peyron et al., 2000; Tillisch et al., 2011). Lateral PFC (represented by the middle frontal gyrus) is typically associated with executive control and attention (Bingel and Tracey, 2008; Lorenz et al., 2003; Wiech et al., 2008), while MI, SMA, and cerebellum have typically been associated with execution of motor responses to avoid pain (Apkarian et al., 2005; Peyron et al., 2000; Moulton et al., 2010). The brainstem receives nociceptive input from the spinal cord and trigeminal nucleus and is also involved in the descending modulation of pain (Basbaum and Fields, 1978; Stamford, 1995), while basal ganglia involvement in pain may reflect modulation of multisensory integration related to pain (Borsook et al., 2010; Chudler and Dong, 1995). We observed convergent amygdala activation in four main effects analyses; the amygdala receives dense projections from nociceptive neurons in the lateral parabrachial nucleus (Jasmin et al., 1997), has been associated with affective modulation of pain and salience detection, and has been reported in both experimental pain and chronic pain experiments (Simons et al., 2014; Borsook et al., 2013; Fernando et al., 2013).

Finally, we did not find consistent involvement of SI in the experimentally-induced pain despite its prior inclusion in a putative “pain matrix” (Iannetti and Mouraux, 2010; Legrain et al., 2011). However, we were able to detect SI involvement in pain in our meta-analyses of left-sided pain and of pain induced in proximal extremities. This less consistent involvement of SI is not surprising; previous reviews have similarly reported less consistent activation of SI in response to painful stimulation compared to other areas (Bushnell et al., 1999; Friebel et al., 2011; Lanz et al., 2011; Peyron et al., 2000). Though SI is known to be critical for the sensory-discriminative aspect of pain (Bushnell et al., 1999; Duerden and Albanese, 2013; Friebel et al., 2011; Peyron et al., 2000), the inconsistency of SI’s specific involvement in pain processing may stem from variable anatomy of SI in individual participants and, more importantly, the precise, localized somatotopic organization of SI (Bushnell et al., 1999). Our results cohere with this interpretation, as SI appeared only in analyses where there was less variability in the stimulation site (e.g., left-sided pain). Considering the highly somatotopic organization of SI, meta-analyses may need to focus on experiments of pain that target precisely the same physical locations of pain induction in order to reliably detect SI activation.

4.3. Differences between experimental pain paradigms

While the predominant pattern of results suggests consistent activation in a core set of regions accompanied by less consistent activation in other areas, we also observed important differences among paradigms. Specifically, we found stronger convergence of activation in right MCC in thermal pain experiments compared to non-thermal pain experiments – a finding consistent with earlier work by Friebe et al. (2011). Given the role of MCC in affective-motivational components of pain (Tracey et al., 2007), our results suggest that thermal experiments may be more affectively-valenced than non-thermal experiments. Notably, our findings indicate a more restricted extent of differences between thermal and non-thermal stimulation than that reported in an earlier meta-analysis by Friebe and colleagues (2011). These differences may be explained in part by the more stringent inclusion criteria and statistical threshold used in our meta-analysis.

We also found differences in the pain response to electrical stimulation compared to mechanical stimulation. Electrical experiments showed stronger convergence of activation in right Rolandic operculum, right thalamus, and right superior temporal gyrus. In contrast, mechanical experiments did not produce greater convergence of activation. These differences, however, are better characterized by a differing extent of convergence of activation rather than different brain areas being recruited. Indeed, we find more widespread significant conjunction of activation between these stimulus modalities than significant differences. Nevertheless, our findings may suggest more robust activation of pain-sensitive brain areas in response to electrical stimulation rather than mechanical stimulation.

The meta-analyses focused on stimulation location primarily revealed a laterality effect. Right-sided pain experiments showed stronger convergence of activation in left SII. However, left-sided pain experiments did not show stronger convergence of activation in right SII. There are currently mixed findings over the extent of contralateral bias in somatotopic encoding in SII (Bingel et al., 2004; Johansen-Berg et al., 2000; Maldjian et al., 1999; Ruben et al., 2001). The stronger convergence of activation in SII may lend support for some contralateral bias in somatotopic encoding of laterality, though further studies are needed to address this more directly. Interestingly, we did not observe differences in our other location-related sub-analyses that focused on proximal versus distal pain and visceral versus non-visceral pain. These findings may suggest that central processing of pain is largely robust to differences in location of pain stimulation.

4.4. Limitations and future directions

Several limitations should be noted. As mentioned above, our findings delineate a convergent set of brain regions recruited across different experimental paradigms of pain, but an explicit meta-analysis of experiments using within-subject contrasts would better elucidate true differences in brain activation between paradigms. Given the limited number of experiments that did explicitly test these differences within-subject, there is great potential for future experiments and meta-analyses to examine differences between experimental paradigms more conclusively. Similarly, because our meta-analysis relied on the published results of past articles, publication bias towards selectively publishing significant findings (and, consequently, difficulty in accounting for unpublished results) may have limited our

findings (Müller et al., 2018). Additionally, it is possible that the wide range of image acquisition parameters in the experiments included may have limited the likelihood of observing some types of effects, particularly if detection sensitivity is related to acquisition parameters (e.g., brainstem, as mentioned in Sclocco et al., 2018). While we cannot exclude the possibility of other regions being more robustly involved in or associated with pain, open sharing of imaging data may allow for better detection of these regions using image-based meta-analytic methods (Salimi-Khorshidi et al., 2009) rather than solely using coordinate-based methods.

5. Conclusion

Convergent results demonstrate that SII, insula, MCC, and thalamus are consistently recruited by acute nociceptive stimuli in healthy subjects across many different experimental paradigms. In contrast, lateral PFC, M1, SMA, cerebellum, brainstem, SI, and the amygdala appear from the current meta-analysis to be more variably involved. Notably, we did not find strong evidence for preferential involvement of any of these brain areas in one specific experimental stimulus paradigm over another. Taken together, these findings suggest that acute pain induction in healthy volunteers consistently recruits a core brain network. If this network overlaps with that which is involved in clinical pain, this “pain biomarker” may offer translational opportunities for fMRI in drug development and in clinical trials.

Supplementary Material

Refer to Web version on PubMed Central for supplementary material.

Acknowledgements

Thank you to Zaixu Cui for his assistance in guidance of surface figure generation.

Funding

This work was supported by the Analgesic, Anesthetic, and Addition Clinical Trial Translations, Innovations, Opportunities, and Networks (ACTION) public-private partnership with the US Food and Drug Administration, which has received research contracts, grants, or other revenue from the FDA, multiple pharmaceutical and device companies, philanthropy, and other sources.

Declaration of Competing Interest

Robert H. Dworkin, PhD, has received in the past 36 months research grants and contracts from the US Food and Drug Administration and the US National Institutes of Health, and compensation for consulting on clinical trial methods from Abide, Acadia, Adynxx, Analgesic Solutions, Aptinyx, Aquinox, Asahi Kasei, Astellas, AstraZeneca, Biogen, Biohaven, Boston Scientific, Braeburn, Celgene, Centrexion, Chromocell, Clexio, Concert, Decibel, Dong-A, Eli Lilly, Eupraxia, Glenmark, Grace, Hope, Immune, Lotus Clinical Research, Mainstay, Neumentum, NeuroBo, Novaremed, Novartis, Olatec, Pfizer, Phosphagenics, Quark, Reckitt Benckiser, Regency (also equity), Relmada, Sanifit, Scilex, Semnur, Sollis, Teva, Theranexus, Trevena, and Vertex.

References

- Ab Aziz CB, Ahmad AH, 2006 The role of the thalamus in modulating pain. *Malays. J. Med. Sci* 13 (2), 11–18. [PubMed: 22589599]
- Apkarian AV, Bushnell MC, Treede R-D, Zubieta J-K, 2005 Human brain mechanisms of pain perception and regulation in health and disease. *Eur. J. Pain* 9 (4). 10.1016/j.ejpain.2004.11.001. 463–463. [PubMed: 15979027]

- Basbaum AI, Fields HL, 1978 Endogenous pain control mechanisms: review and hypothesis. *Ann. Neurol* 4 (5), 451–462. 10.1002/ana.410040511. [PubMed: 216303]
- Behrens TEJ, Johansen-Berg H, Woolrich MW, Smith SM, Wheeler-Kingshott CA, Behrens TEJ, Johansen-Berg H, Woolrich MW, Smith SM, Wheeler-Kingshott CAM, Boulby PA, et al., 2003 Non-invasive mapping of connections between human thalamus and cortex using diffusion imaging. *Nat. Neurosci* 6 (7), 8.
- Bingel U, Lorenz J, Glauche V, Knab R, Gläscher J, Weiller C, Büchel C, 2004. Somatotopic Organization of human somatosensory cortices for pain: a single trial fMRI study. *NeuroImage* 23 (1), 224–232. 10.1016/j.neuroimage.2004.05.021. [PubMed: 15325369]
- Bingel U, Tracey I, 2008. Imaging CNS modulation of pain in humans. *Physiology* 23 (6), 371–380. 10.1152/physiol.00024.2008. [PubMed: 19074744]
- Borsook D, Upadhyay J, Chudler EH, Becerra L, 2010 A Key Role of the Basal Ganglia in Pain and Analgesia - Insights Gained Through Human Functional Imaging. pp. 17.
- Bushnell MC, Duncan GH, Hofbauer RK, Ha B, Chen J-I, Carrier B, 1999 Pain perception: is there a role for primary somatosensory cortex? *Proc. Natl. Acad. Sci* 96 (14), 7705–7709. 10.1073/pnas.96.14.7705. [PubMed: 10393884]
- Caspers S, Zilles K, Laird AR, Eickhoff SB, 2010. ALE meta-analysis of action observation and imitation in the human brain. *NeuroImage* 50 (3), 1148–1167. 10.1016/j.neuroimage.2009.12.112. [PubMed: 20056149]
- Chen TL, Babiloni C, Ferretti A, Perrucci MG, Romani GL, Rossini PM, et al., 2008 Human secondary somatosensory cortex is involved in the processing of somatosensory rare stimuli: an fMRI study. *NeuroImage* 40 (4), 1765–1771. 10.1016/j.neuroimage.2008.01.020. [PubMed: 18329293]
- Chudler EH, Dong WK, 1995 The role of the basal ganglia in nociception and pain. *Pain* 60 (1), 3–38. 10.1016/0304-3959(94)00172-B. [PubMed: 7715939]
- Cieslik EC, Seidler I, Laird AR, Fox PT, Eickhoff SB, 2016 Different involvement of subregions within dorsal premotor and medial frontal cortex for pro- and anti-saccades. *Neurosci. Biobehav. Rev* 68, 256–269. 10.1016/j.neubiorev.2016.05.012. [PubMed: 27211526]
- Cowen R, Stasiowska MK, Laycock H, Bantel C, 2015 Assessing pain objectively: the use of physiological markers. *Anaesthesia* 70 (7), 828–847. 10.1111/anae.13018. [PubMed: 25772783]
- Craig AD, 2009 How do you feel—now? The anterior insula and human awareness. *Nat. Rev. Neurosci* 10 (1), 59–70. 10.1038/nrn2555. [PubMed: 19096369]
- Craig AD, Chen K, Bandy D, Reiman EM, 2000 Thermosensory activation of insular cortex. *Nat. Neurosci* 3 (2), 184–190. 10.1038/72131. [PubMed: 10649575]
- Duerden EG, Albanese MC, 2013 Localization of pain-related brain activation: a meta-analysis of neuroimaging data. *Hum. Brain Mapp* 34 (1), 109–149. 10.1002/hbm.21416. [PubMed: 22131304]
- Eickhoff SB, Stephan KE, Mohlberg H, Grefkes C, Fink GR, Amunts K, Zilles K, 2005 A new SPM toolbox for combining probabilistic cytoarchitectonic maps and functional imaging data. *NeuroImage* 25 (4), 1325–1335. 10.1016/j.neuroimage.2004.12.034. [PubMed: 15850749]
- Eickhoff SB, Laird AR, Grefkes C, Wang LE, Zilles K, Fox PT, 2009 Coordinate-based activation likelihood estimation meta-analysis of neuroimaging data: a random-effects approach based on empirical estimates of spatial uncertainty. *Hum. Brain Mapp* 30 (9), 2907–2926. 10.1002/hbm.20718. [PubMed: 19172646]
- Eickhoff SB, Bzdok D, Laird AR, Kurth F, Fox PT, 2012 Activation likelihood estimation meta-analysis revisited. *NeuroImage* 59 (3), 2349–2361. 10.1016/j.neuroimage.2011.09.017. [PubMed: 21963913]
- Eickhoff SB, Nichols TE, Laird AR, Hoffstaedter F, Amunts K, Fox PT, et al., 2016 Behavior, sensitivity, and power of activation likelihood estimation characterized by massive empirical simulation. *NeuroImage* 137, 70–85. 10.1016/j.neuroimage.2016.04.072. [PubMed: 27179606]
- Eklund A, Nichols T, Knutsson H, 2016 Can parametric statistical methods be trusted for fMRI based group studies? *Proc. Natl. Acad. Sci* 113 (28), 7900–7905. 10.1073/pnas.1602413113. [PubMed: 27357684]

- Farrell MJ, Laird AR, Egan GF, 2005 Brain activity associated with painfully hot stimuli applied to the upper limb: a meta-analysis. *Hum. Brain Mapp* 25 (1), 129–139. 10.1002/hbm.20125. [PubMed: 15846813]
- Ferretti A, Babiloni C, Gratta CD, Caulo M, Tartaro A, Bonomo L, et al., 2003 Functional topography of the secondary somatosensory cortex for nonpainful and painful stimuli: an fMRI study. *NeuroImage* 20 (3), 1625–1638. 10.1016/j.neuroimage.2003.07.004. [PubMed: 14642473]
- Fernando AB, Murray JE, Milton AL, 2013 The amygdala: securing pleasure and avoiding pain. *Front. Behav. Neurosci* 7 10.3389/fnbeh.2013.00190.
- Friebel U, Eickhoff SB, Lotze M, 2011. Coordinate-based meta-analysis of experimentally induced and chronic persistent neuropathic pain. *NeuroImage* 58 (4), 1070–1080. 10.1016/j.neuroimage.2011.07.022. [PubMed: 21798355]
- Goldberg DS, McGee SJ, 2011 Pain as a global public health priority. *BMC Public Health* 11 (1), 770 10.1186/1471-2458-11-770. [PubMed: 21978149]
- Hofbauer RK, Rainville P, Duncan GH, Bushnell MC, 2001. Cortical representation of the sensory dimension of pain. *J. Neurophysiol* 86 (1), 402–411. 10.1152/jn.2001.86.1.402. [PubMed: 11431520]
- Iannetti GD, Mouraux A, 2010 From the neuromatrix to the pain matrix (and back). *Exp. Brain Res* 205 (1), 1–12. 10.1007/s00221-010-2340-1. [PubMed: 20607220]
- Isnard J, Magnin M, Jung J, Mauguière F, Garcia-Larrea L, 2011. Does the insula tell our brain that we are in pain? *Pain* 152 (4), 946–951. 10.1016/j.pain.2010.12.025. [PubMed: 21277680]
- Jasmin L, Burkey AR, Card JP, Basbaum AI, 1997 Transneuronal labeling of a nociceptive pathway, the spino-(Trigemino-)Parabrachio-Amygdaloid, in the rat. *J. Neurosci* 17 (10), 3751–3765. 10.1523/JNEUROSCI.17-10-03751.1997. [PubMed: 9133395]
- Jensen KB, Regenbogen C, Ohse MC, Frasnelli J, Freiherr J, Lundström JN, 2016 Brain activations during pain: a neuroimaging meta-analysis of patients with pain and healthy controls. *Pain* 157 (6), 1279–1286. 10.1097/j.pain.0000000000000517. [PubMed: 26871535]
- Johansen-Berg H, Christensen V, Woolrich M, Matthews PM, 2000 Attention to touch modulates activity in both primary and secondary somatosensory areas. *NeuroReport* 11 (6), 1237–1241. [PubMed: 10817599]
- Kennedy DN, Lange N, Makris N, Bates J, Meyer J, Caviness VS, 1998. Gyri of the human neocortex: an MRI-based analysis of volume and variance. *Cerebral Cortex (New York, N.Y.: 1991)* 8 (4), 372–384. 10.1093/cercor/8.4.372.
- Kurth F, Zilles K, Fox PT, Laird AR, Eickhoff SB, 2010 A link between the systems: functional differentiation and integration within the human insula revealed by meta-analysis. *Brain Struct. Funct* 214 (5–6), 519–534. 10.1007/s00429-010-0255-z. [PubMed: 20512376]
- Labus JS, Van Horn JD, Gupta A, Alaverdyan M, Torgerson C, Ashe-McNalley C, et al., 2015 Multivariate morphological brain signatures predict patients with chronic abdominal pain from healthy control subjects. *Pain*. 10.1097/j.pain.0000000000000196.
- Laird AR, Lancaster JL, Fox PT, 2005 BrainMap: the social evolution of a functional neuroimaging database. *Neuroinformatics* 3, 65–78. [PubMed: 15897617]
- Lancaster JL, Tordesillas-Gutiérrez D, Martínez M, Salinas F, Evans A, Zilles K, et al., 2007 Bias between MNI and Talairach coordinates analyzed using the ICBM-152 brain template. *Hum. Brain Mapp* 28 (11), 1194–1205. 10.1002/hbm.20345. [PubMed: 17266101]
- Lanz S, Seifert F, Maihöfner C, 2011 Brain activity associated with pain, hyperalgesia and allodynia: an ALE meta-analysis. *J. Neural Transm* 118 (8), 1139–1154. 10.1007/s00702-011-0606-9. [PubMed: 21373762]
- Legrain V, Iannetti GD, Plaghki L, Mouraux A, 2011. The pain matrix reloaded. *Prog. Neurobiol* 93 (1), 111–124. 10.1016/j.pneurobio.2010.10.005. [PubMed: 21040755]
- Lorenz J, Minoshima S, Casey KL, 2003 Keeping pain out of mind: the role of the dorsolateral prefrontal cortex in pain modulation. *Brain* 126 (5), 1079–1091. 10.1093/brain/awg102. [PubMed: 12690048]
- Maldjian JA, Gottschalk A, Patel RS, Pincus D, Detre JA, Alsop DC, 1999 Mapping of the secondary somatosensory cortex activation induced by vibrational stimulation: an fMRI study. *Brain Res.* 824 (2), 291–295. 10.1016/S0006-8993(99)01126-9. [PubMed: 10196461]

- Mazzola L, Isnard J, Mauguière F, 2006 Somatosensory and pain responses to stimulation of the second somatosensory area (SII) in humans. A comparison with SI and insular responses. *Cereb. Cortex* 16 (7), 960–968. 10.1093/cercor/bhj038. [PubMed: 16177270]
- Medford N, Critchley HD, 2010 Conjoint activity of anterior insular and anterior cingulate cortex: awareness and response. *Brain Struct. Funct* 214 (5–6), 535–549. 10.1007/s00429-010-0265-x. [PubMed: 20512367]
- Menon V, Uddin LQ, 2010 Saliency, switching, attention and control: a network model of insula function. *Brain Struct. Funct* 214 (5), 655–667. 10.1007/s00429-010-0262-0. [PubMed: 20512370]
- Moher D, Liberati A, Tetzlaff J, Altman DG, Group TP, 2009 Preferred reporting items for systematic reviews and meta-analyses: the PRISMA statement. *PLoS Med.* 6 (7), e1000097. 10.1371/journal.pmed.1000097.
- Morrison A, Polisena J, Husereau D, Moulton K, Clark M, Fiander M, Mierzwinski-Urban M, Clifford T, Hutton B, Rabb D, 2012 The effect of English-language restriction on systematic review-based meta-analyses: a systematic review of empirical studies. *Int. J. Technol. Assess. Health Care* 28, 138–144. [PubMed: 22559755]
- Moulton EA, Schmahmann JD, Becerra L, Borsook D, 2010. The cerebellum and pain: passive integrator or active participant? *Brain Res. Rev* 65 (1), 14–27. 10.1016/j.brainresrev.2010.05.005. [PubMed: 20553761]
- Müller VI, Cieslik EC, Laird AR, Fox PT, Radua J, Mataix-Cols D, et al., 2018 Ten simple rules for neuroimaging meta-analysis. *Neurosci. Biobehav. Rev* 84, 151–161. 10.1016/j.neubiorev.2017.11.012. [PubMed: 29180258]
- Nichols T, Brett M, Andersson J, Wager T, Poline J-B, 2005 Valid conjunction inference with the minimum statistic. *NeuroImage* 25 (3), 653–660. 10.1016/j.neuroimage.2004.12.005. [PubMed: 15808966]
- Peyron R, Laurent B, García-Larrea L, 2000 Functional imaging of brain responses to pain. A review and meta-analysis (2000). *Neurophysiol. Clin. Neurophysiol* 30 (5), 263–288. 10.1016/S0987-7053(00)00227-6.
- Robinson ME, Staud R, Price DD, 2013 Pain Measurement and Brain Activity: Will Neuroimages Replace Pain Ratings? *J. Pain* 14 (4), 323–327. 10.1016/j.jpain.2012.05.007. [PubMed: 23548484]
- Rottschy C, Langner R, Dogan I, Reetz K, Laird AR, Schulz JB, et al., 2012 Modelling neural correlates of working memory: a coordinate-based meta-analysis. *NeuroImage* 60 (1), 830–846. 10.1016/j.neuroimage.2011.11.050. [PubMed: 22178808]
- Ruben J, Schwiemann J, Deuchert M, Meyer R, Krause T, Curio G, Villringer K, Kurth R, Villringer A, 2001 Somatotopic organization of human secondary somatosensory cortex. *Cereb. Cortex* 11 (5), 462–473. 10.1093/cercor/11.5.463.
- Salimi-Khorshidi G, Smith SM, Keltner JR, Wager TD, Nichols TE, 2009 Meta-analysis of neuroimaging data: a comparison of image-based and coordinate-based pooling of studies. *NeuroImage* 45 (3), 810–823. 10.1016/j.neuroimage.2008.12.039. [PubMed: 19166944]
- Sclocco R, Beissner F, Bianciardi M, Polimeni JR, Napadow V, 2018 Challenges and opportunities for brainstem neuroimaging with ultrahigh field MRI. *NeuroImage* 168, 412–426. 10.1016/j.neuroimage.2017.02.052. [PubMed: 28232189]
- Shackman AJ, Salomons TV, Slagter HA, Fox AS, Winter JJ, Davidson RJ, 2011 The integration of negative affect, pain and cognitive control in the cingulate cortex. *Nat. Rev. Neurosci* 12 (3), 154–167. 10.1038/nrn2994. [PubMed: 21331082]
- Simons LE, Moulton EA, Linnman C, Carpino E, Becerra L, Borsook D, 2014 The human amygdala and pain: evidence from neuroimaging. *Hum. Brain Mapp* 35 (2), 527–538. 10.1002/hbm.22199. [PubMed: 23097300]
- Stamford JA, 1995 Descending control of pain. *Br. J. Anaesth* 75 (2), 217–227. 10.1093/bja/75.2.217. [PubMed: 7577256]
- Taylor KS, Seminowicz DA, Davis KD, 2009 Two systems of resting state connectivity between the insula and cingulate cortex. *Hum. Brain Mapp* 30 (9), 2731–2745. 10.1002/hbm.20705. [PubMed: 19072897]

- Talbot J, Marrett S, Evans A, Meyer E, Bushnell M, Duncan G, 1991 Multiple representations of pain in human cerebral cortex. *Science* 251 (4999), 1355–1358. 10.1126/science.2003220. [PubMed: 2003220]
- Tanasescu R, Cottam WJ, Condon L, Tench CR, Auer DP, 2016 Functional reorganisation in chronic pain and neural correlates of pain sensitisation: a coordinate based meta-analysis of 266 cutaneous pain fMRI studies. *Neurosci. Biobehav. Rev* 68, 120–133. 10.1016/j.neubiorev.2016.04.001. [PubMed: 27168346]
- Tillisch K, Mayer EA, Labus JS, 2011. Quantitative meta-analysis identifies brain regions activated during rectal distension in irritable bowel syndrome. *Gastroenterology* 140 (1), 91–100. 10.1053/j.gastro.2010.07.053. [PubMed: 20696168]
- Toro R, 2015 Brainspell. [<http://brainspell.org>].
- Tracey I, Mantyh PW, 2007. The cerebral signature for pain perception and its modulation. *Neuron* 55 (3), 377–391. 10.1016/j.neuron.2007.07.012. [PubMed: 17678852]
- Treede R-D, Kenshalo DR, Gracely RH, Jones AKP, 1999 The cortical representation of pain. *Pain* 79 (2), 105–111. 10.1016/S0304-3959(98)00184-5. [PubMed: 10068155]
- Turkeltaub PE, Eden GF, Jones KM, Zeffiro TA, 2002 Meta-analysis of the functional neuroanatomy of single-word reading: method and validation. *NeuroImage* 16 (3, Part A), 765–780. 10.1006/nimg.2002.1131. [PubMed: 12169260]
- Turkeltaub PE, Eickhoff SB, Laird AR, Fox M, Wiener M, Fox P, 2012 Minimizing within-experiment and within-group effects in activation likelihood estimation meta-analyses. *Hum. Brain Mapp* 33 (1), 1–13. 10.1002/hbm.21186. [PubMed: 21305667]
- Vogt BA, 2005 Pain and emotion interactions in subregions of the cingulate gyrus. *Nat. Rev. Neurosci* 6 (7), 533–544. 10.1038/nrn1704. [PubMed: 15995724]
- Vogt BA, 2016 Midcingulate cortex: structure, connections, homologies, functions and diseases. *J. Chem. Neuroanat* 74, 28–46. 10.1016/j.jchemneu.2016.01.010. [PubMed: 26993424]
- Vogt BA, Berger GR, Derbyshire SWG, 2003. Structural and functional dichotomy of human midcingulate cortex. *Eur. J. Neurosci* 18 (11), 3134–3144. 10.1111/j.1460-9568.2003.03034.x. [PubMed: 14656310]
- Wager TD, Lindquist MA, Nichols TE, Kober H, Van Snellenberg JX, 2009 Evaluating the consistency and specificity of neuroimaging data using meta-analysis. *NeuroImage* 45 (1, Supplement 1), S210–S221. 10.1016/j.neuroimage.2008.10.061. [PubMed: 19063980]
- Wager TD, Atlas LY, Lindquist MA, Roy M, Woo C-W, Kross E, 2013 An fMRI-Based neurologic signature of physical pain. *N. Engl. J. Med* 10.1056/NEJMoa1204471.
- Wiech K, Ploner M, Tracey I, 2008. Neurocognitive aspects of pain perception. *Trends Cogn. Sci* 12 (8), 306–313. 10.1016/j.tics.2008.05.005. [PubMed: 18606561]
- Woo C-W, Chang LJ, Lindquist MA, Wager TD, 2017 Building better biomarkers: brain models in translational neuroimaging. *Nat. Neurosci* 20 (3), 365–377. 10.1038/nn.4478. [PubMed: 28230847]
- Woo C-W, Wager TD, 2016 What reliability can and cannot tell us about pain report and pain neuroimaging. *Pain* 157 (3), 511–513. 10.1097/j.pain.0000000000000442. [PubMed: 26645548]
- Yarkoni T, Poldrack RA, Nichols TE, Van Essen DC, Wager TD, 2011 Large-scale automated synthesis of human functional neuroimaging data. *Nat. Methods* 8 (8), 665–670. 10.1038/nmeth.1635. [PubMed: 21706013]
- Yen C-T, Lu P-L, 2013 Thalamus and pain. *Acta Anaesthesiol. Taiwanica* 51 (2), 73–80. 10.1016/j.aat.2013.06.011.

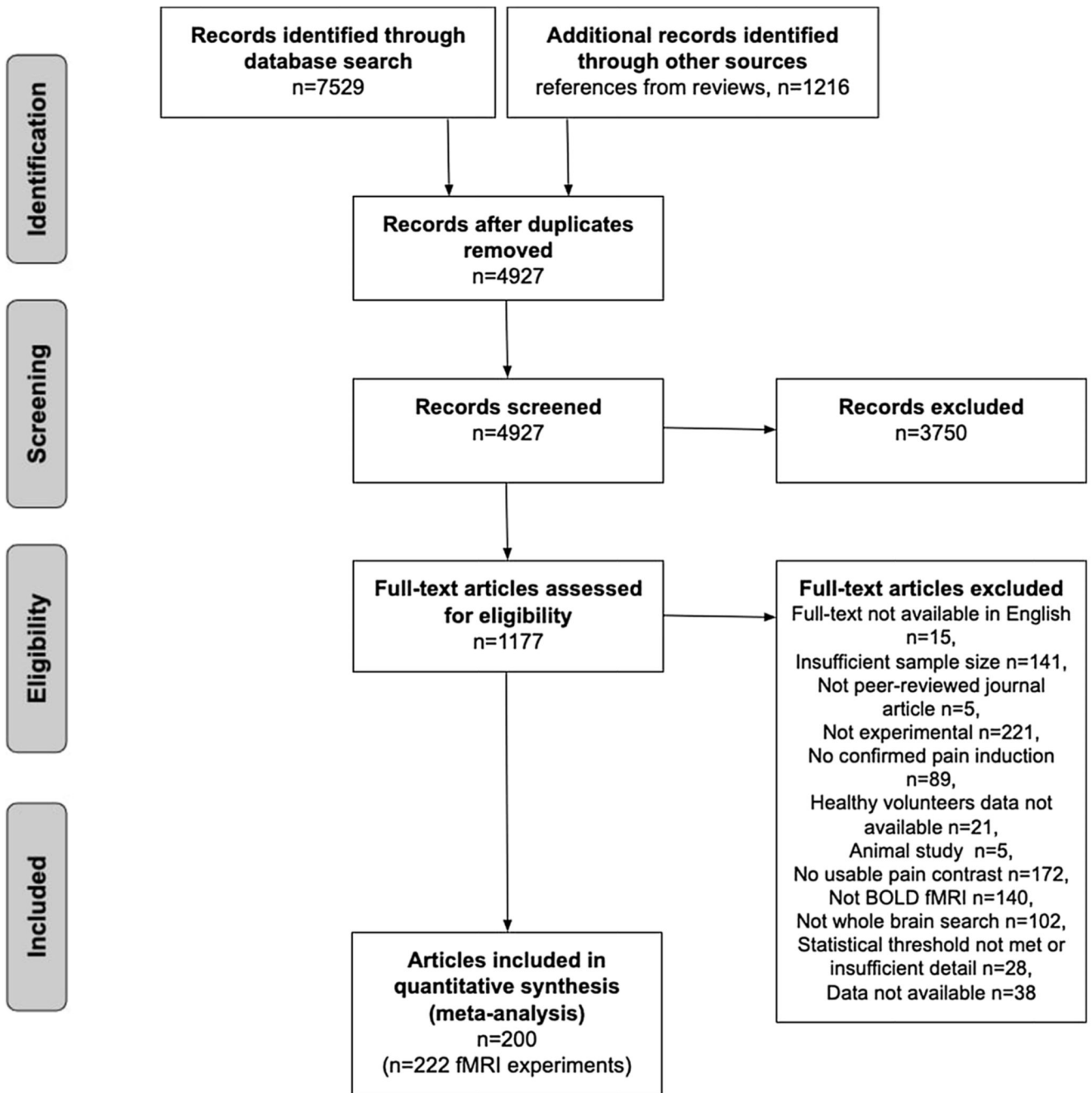


Fig. 1.
PRISMA flowchart for study inclusion.

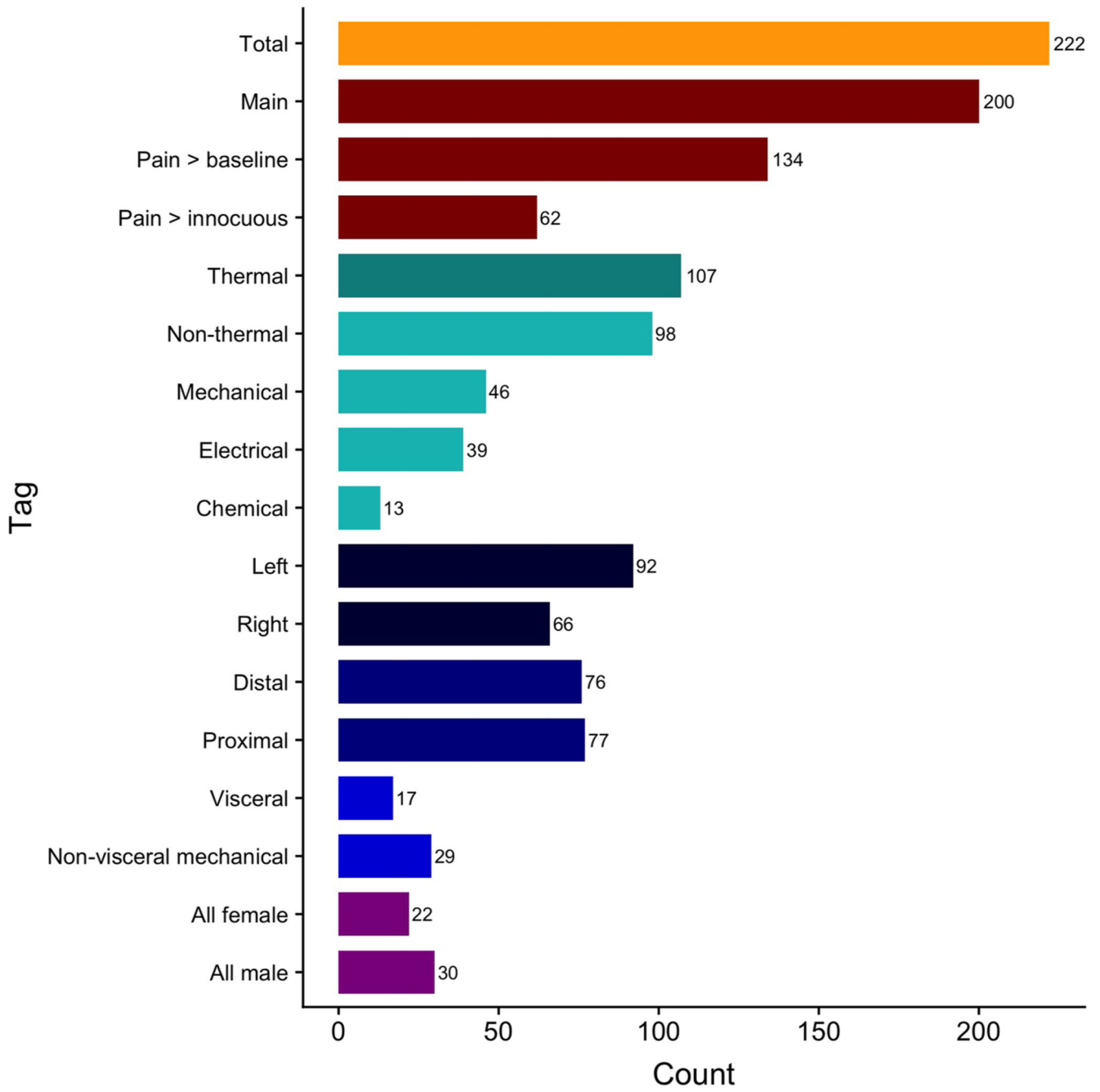


Fig. 2.
 Number of experiments included in each analysis of interest.

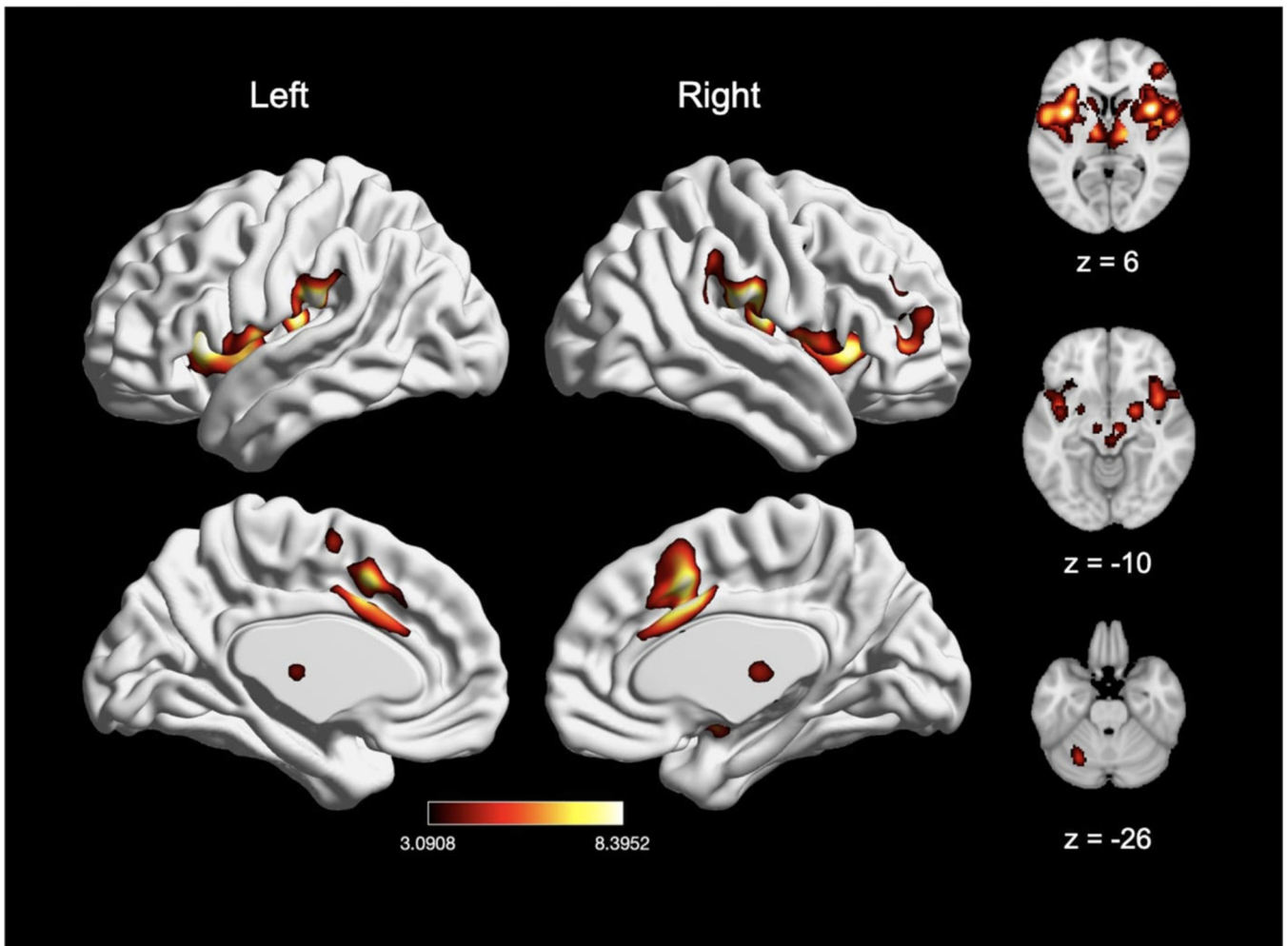


Fig. 3. Main effect of experimental induction of acute pain (n = 200). Coordinates and statistics for significant clusters are shown in Table 2.

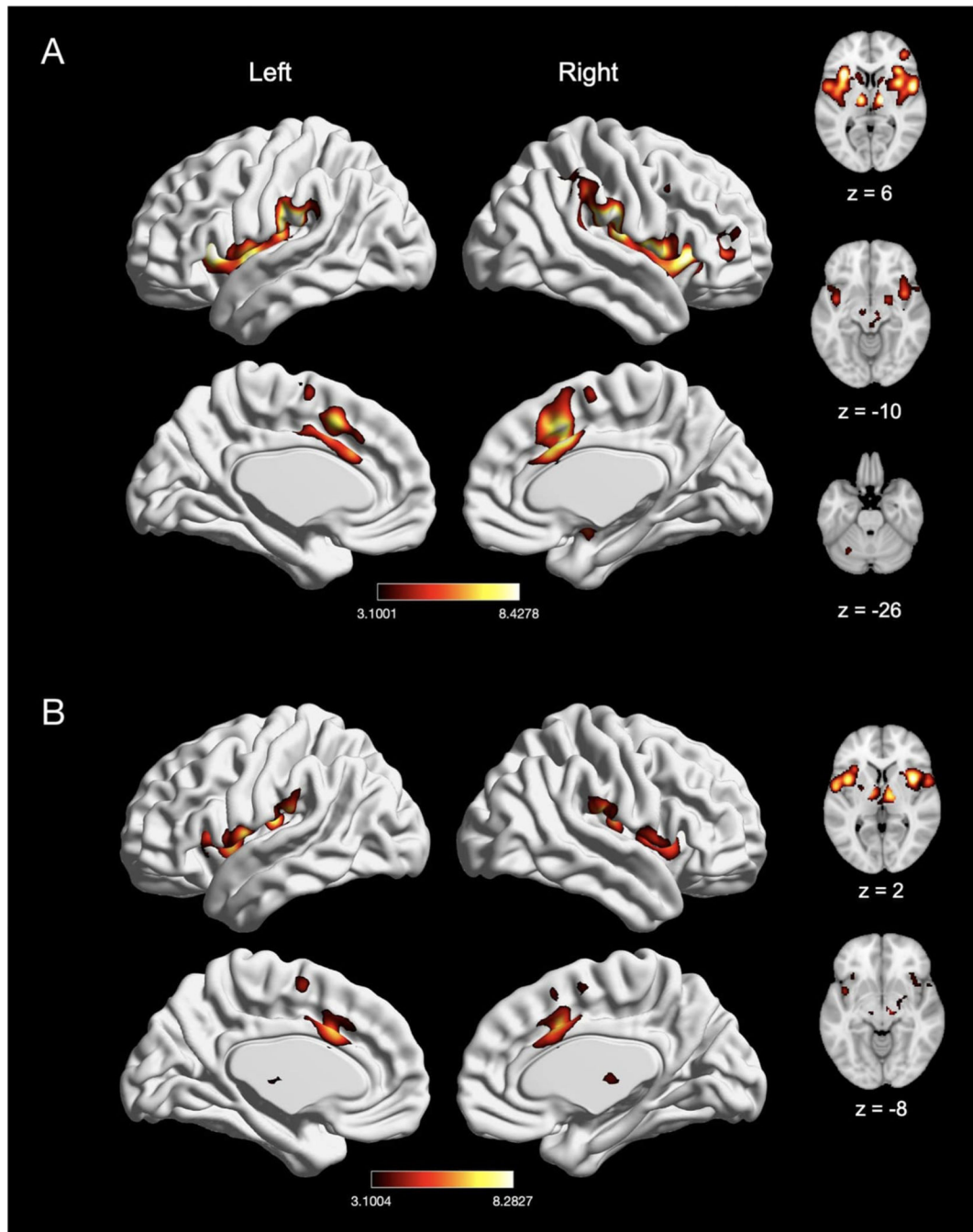


Fig. 4. Meta-analytic effect of experiments using “pain > rest” and “pain > innocuous” contrast. (A) Main effect of experiments using “pain > rest” contrast ($n = 134$). (B) Main effect of experiments with “pain > innocuous” contrast ($n = 62$). Coordinates and statistics for significant clusters are shown in Table 3.

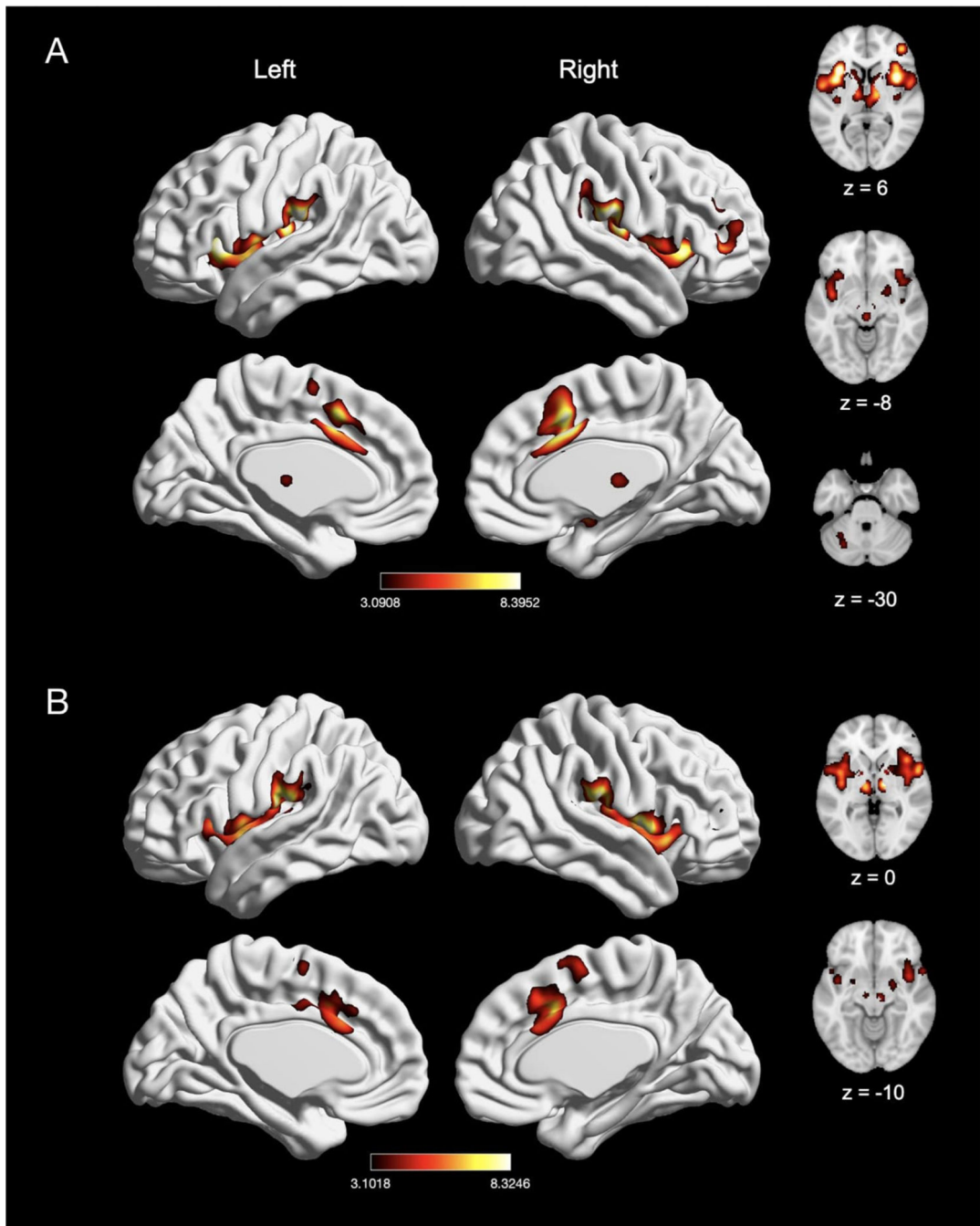


Fig. 5. The meta-analytic effects of thermal and non-thermal nociceptive pain induction. (A) Main effect of thermal pain experiments ($n = 107$). (B) Main effect of non-thermal pain experiments ($n = 98$). Coordinates and statistics for significant clusters associated with the main effect of thermal and non-thermal pain (as well as the between-experiment contrast and conjunction of thermal and non-thermal pain experiments) are shown in Table 4.

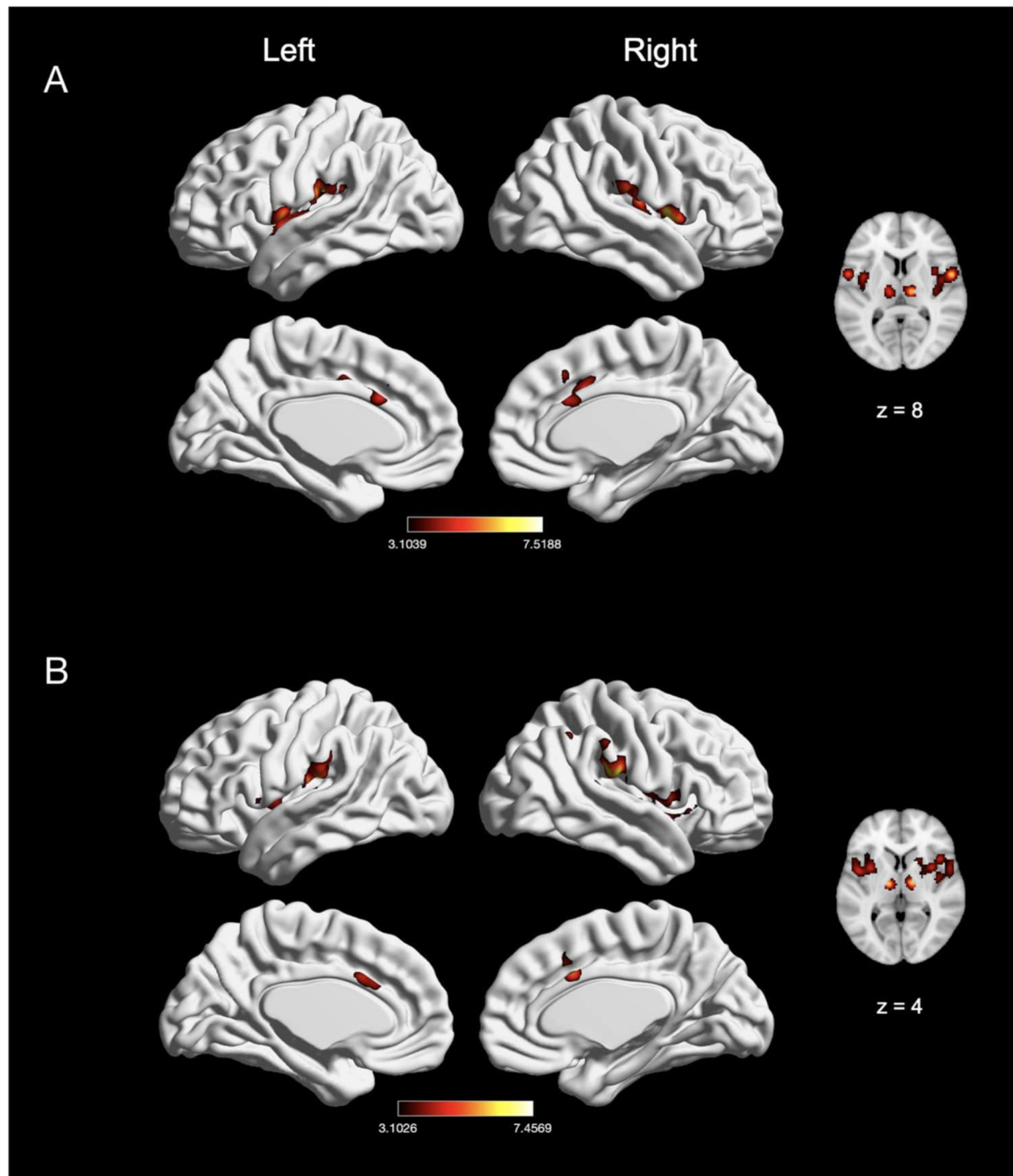


Fig. 6. Effects of induction of electrically-evoked and mechanical nociceptive pain. (A) Main effect of electrically-evoked pain experiments ($n = 39$). (B) Main effect of mechanical pain experiments ($n = 46$). Coordinates and statistics for significant clusters associated with the main effect of electrical and mechanical pain (as well as the between-experiment contrast and conjunction of electrical and mechanical pain experiments) are shown in Table 5.

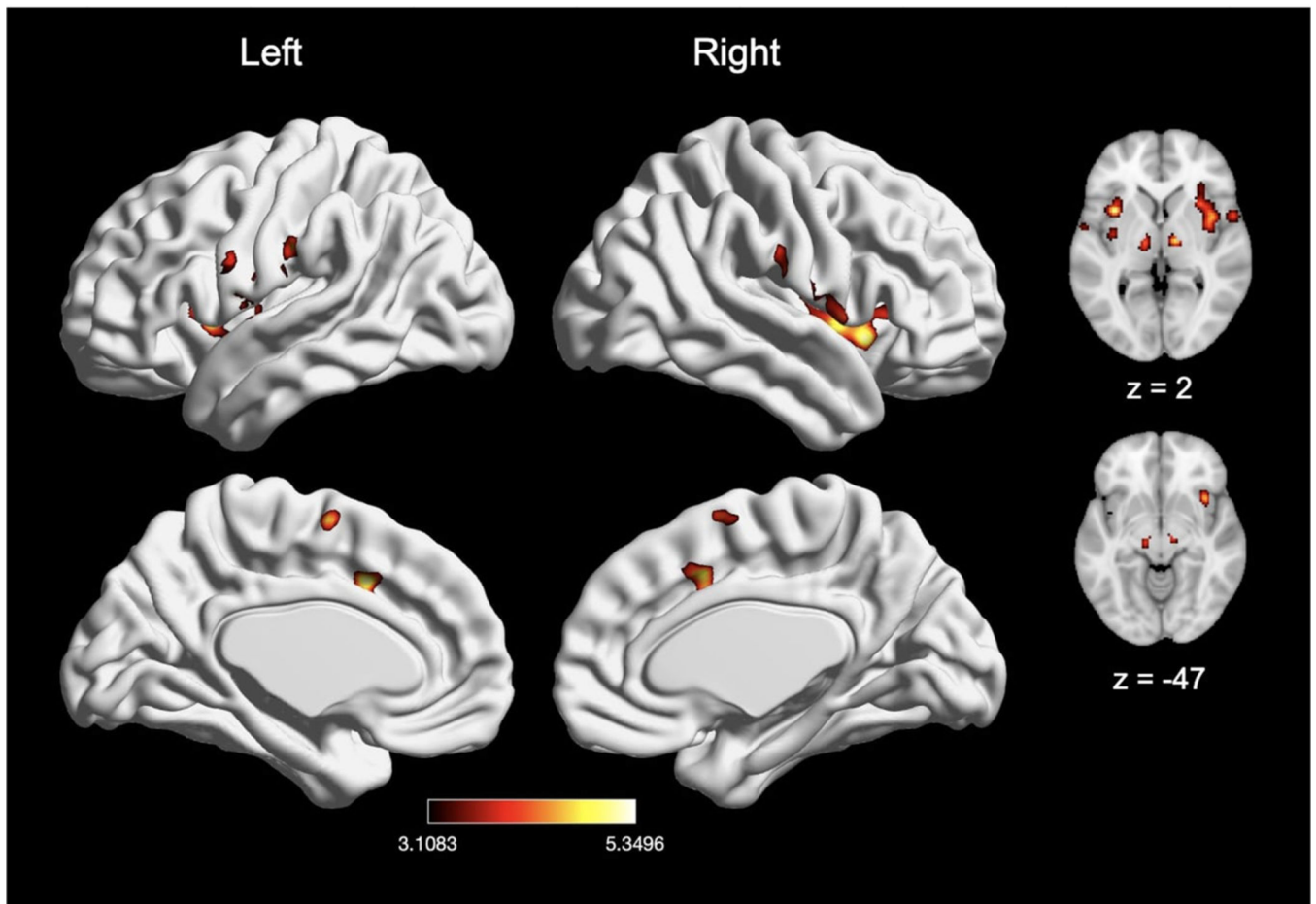


Fig. 7. Main effect of meta-analysis of nociceptive chemical pain experiments ($n = 13$). Coordinates and statistics for significant clusters associated with the main effect of chemical pain are shown in Table 6.

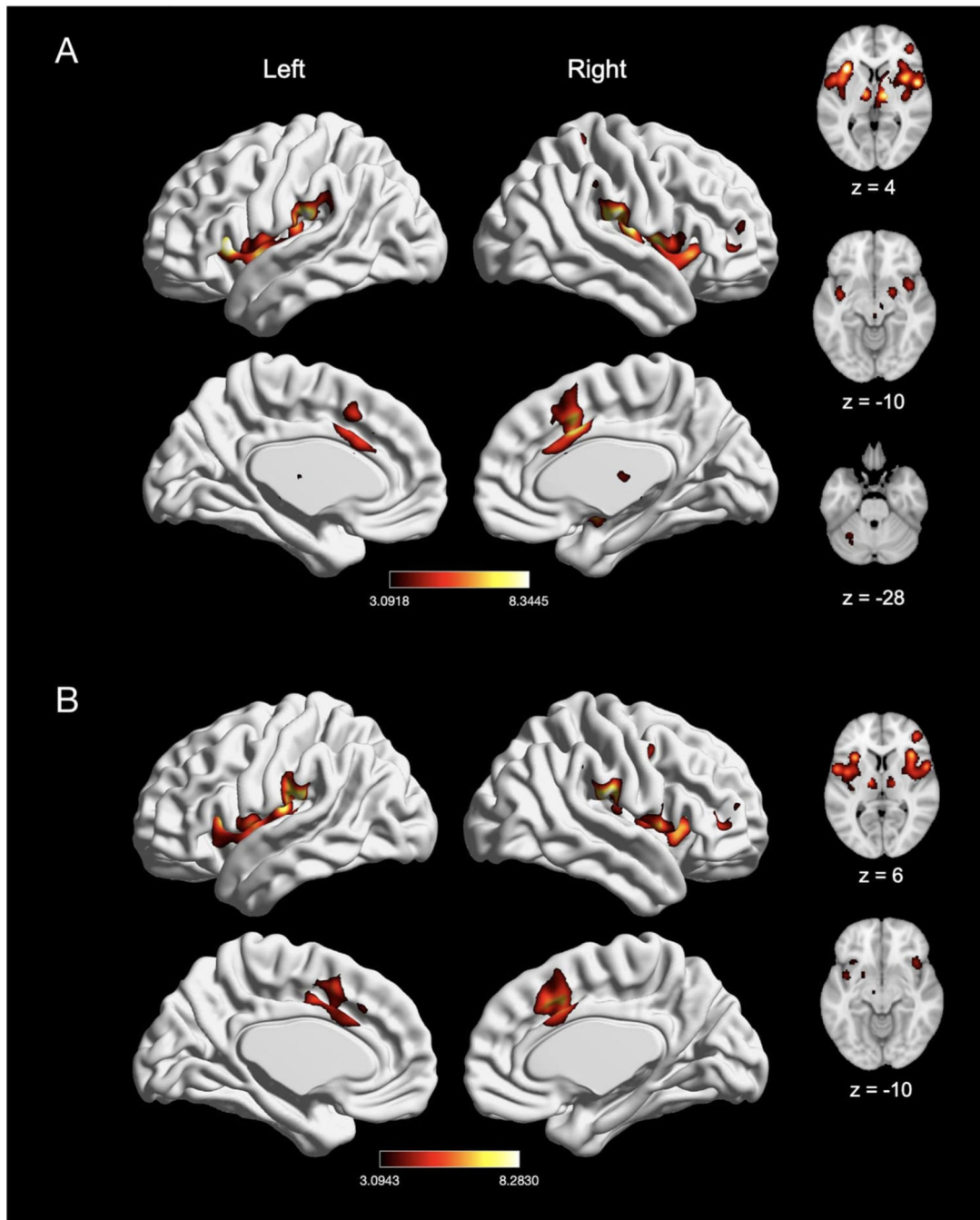


Fig. 8. The meta-analytic effects of left-sided and right-sided pain induction. (A) Main effect of left-sided pain experiments ($n = 92$). (B) Main effect of right-sided pain experiments ($n = 66$). Coordinates and statistics for significant clusters associated with the main effect of left-sided and right-sided pain (as well as the between-experiment contrast and conjunction of left-sided and right-sided pain experiments) are shown in Table 7.

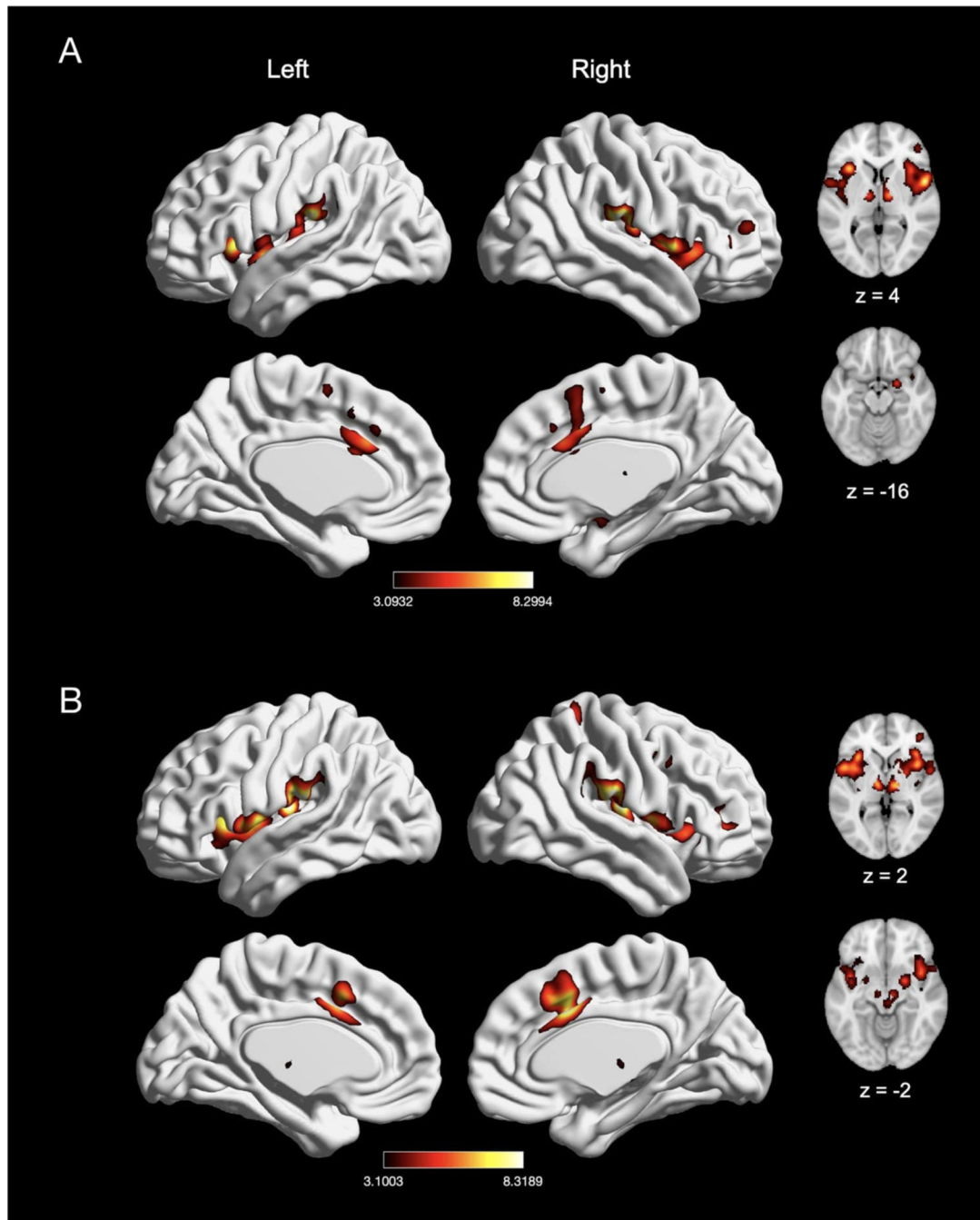


Fig. 9. The meta-analytic effects of distal and proximal nociceptive pain. (A) Main effect of experiments inducing acute nociceptive pain in the distal extremities ($n = 68$). (B) Main effect of experiments inducing pain in the proximal extremities ($n = 85$). Coordinates and statistics for significant clusters associated with the main effect of distal and proximal pain (as well as the between-experiment contrast and conjunction of distal and proximal pain experiments) are shown in Table 8.

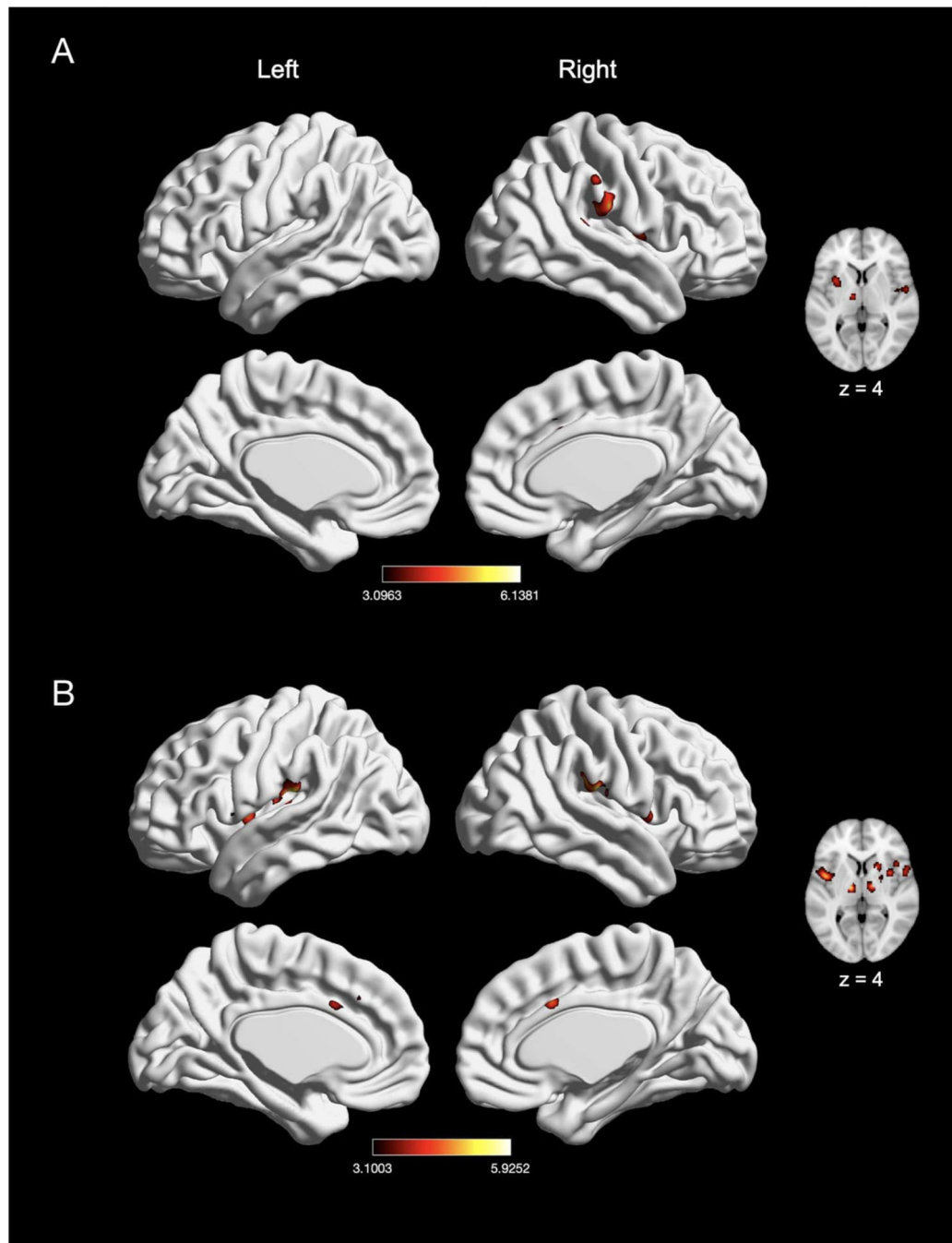


Fig. 10. The meta-analytic effects of visceral and non-visceral mechanical pain. (A) Main effect of visceral pain experiments ($n = 17$). (B) Main effect of non-visceral mechanical pain experiments ($n = 29$). Coordinates and statistics for significant clusters associated with the main effect of visceral and non-visceral pain (as well as the between-experiment contrast and conjunction of visceral and non-visceral pain experiments) are shown in Table 9.

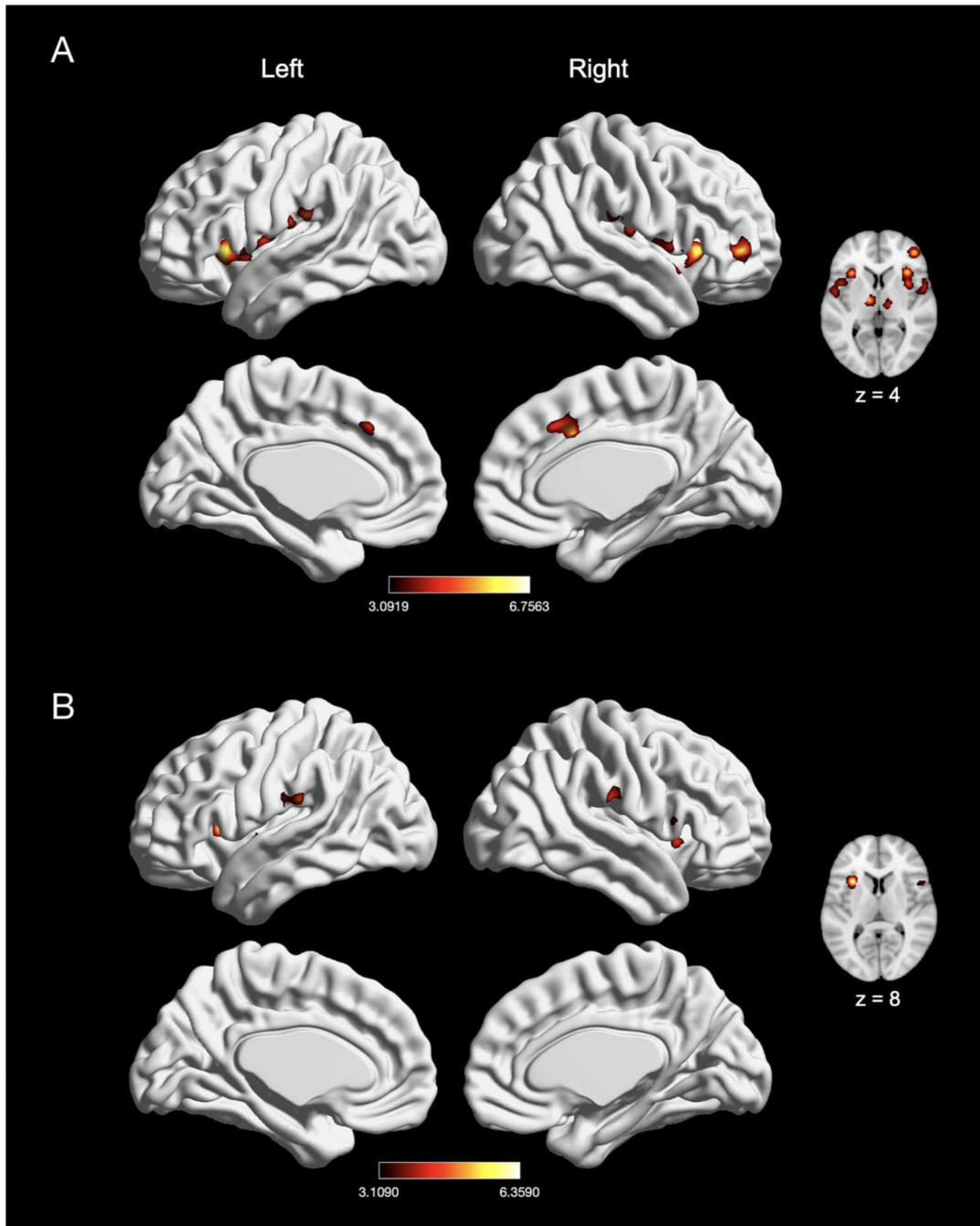


Fig. 11. Effect of pain in males and females. (A) Main effect of experiments with an all-female sample ($n = 22$). (B) Main effect of experiments with an all-male sample ($n = 30$). Coordinates and statistics for significant clusters are shown in Table 10.

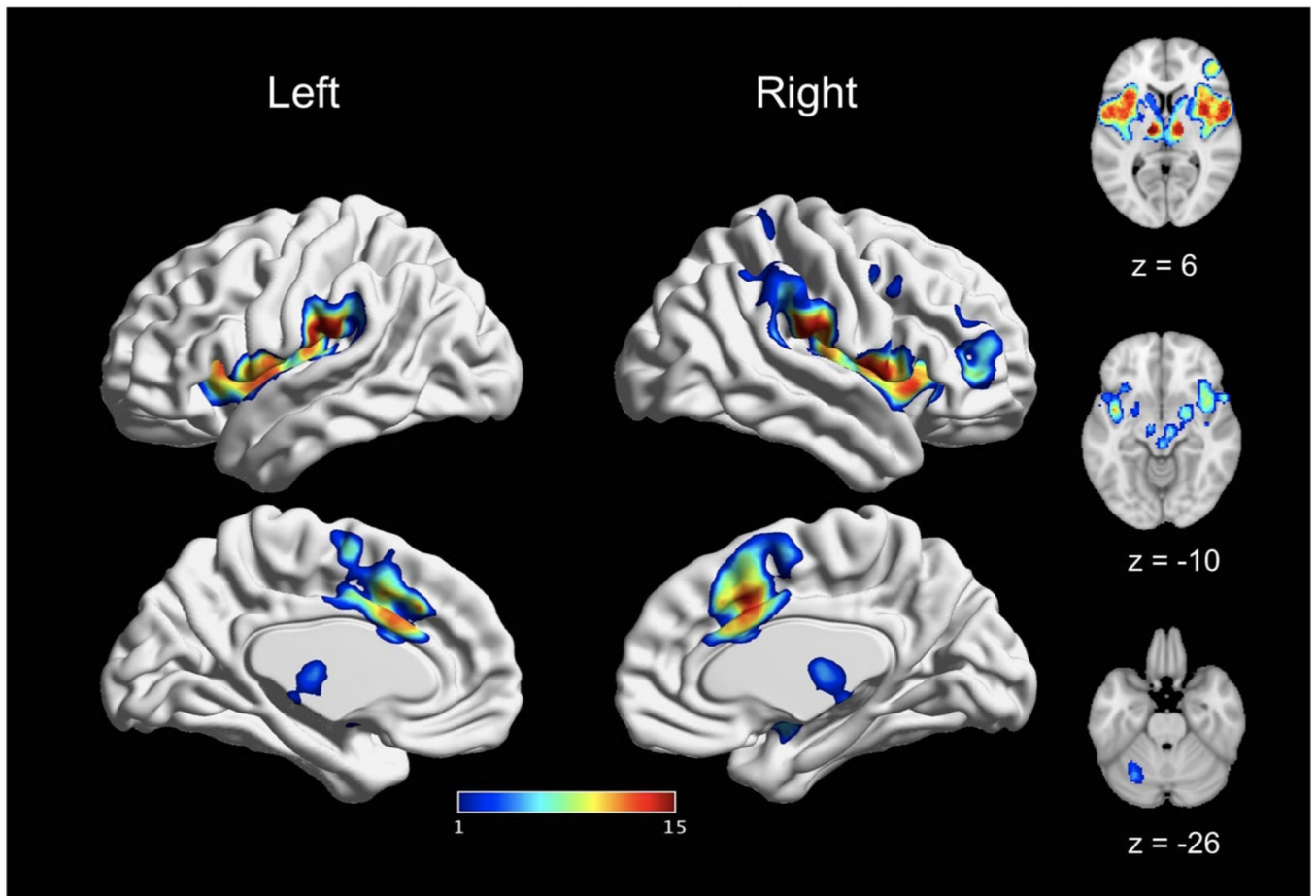


Fig. 12.

A core set of brain regions recruited by acute pain. This figure depicts the spatial consistency of above-threshold activation convergence across all reported main effects meta-analyses. The value assigned to each voxel reflects the number of main effects analyses in which it was reported as significant. Values range from 1 (reported significant in only one main effects meta-analyses) to 15 (reported as significant in all main effects meta-analyses). The most consistently activated areas include bilateral thalamus, bilateral insula, bilateral SII, and bilateral MCC.

Table 1

Number of experiments included and number of participants for each effect of interest.

| Effect of interest | <i>n</i> | Total number of participants | Average number of participants |
|---|----------|------------------------------|--------------------------------|
| <i>Noiceptive Pain</i> | | | |
| All pain | 200 | 3816 | 19 |
| Pain > innocuous | 62 | 1202 | 19 |
| Pain > rest | 134 | 2547 | 19 |
| <i>Modality</i> | | | |
| Thermal | 107 | 2083 | 19 |
| Non-thermal | 98 | 1801 | 18 |
| Electrical | 39 | 755 | 19 |
| Mechanical | 46 | 788 | 17 |
| Chemical | 13 | 258 | 20 |
| <i>Location</i> | | | |
| Side | | | |
| Left | 92 | 1873 | 20 |
| Right | 66 | 1214 | 18 |
| <i>Distal vs. Proximal Extremities</i> | | | |
| Distal (hand or foot) | 68 | 1254 | 18 |
| Proximal (arm or leg) | 85 | 1764 | 21 |
| <i>Visceral vs. Non-visceral mechanical</i> | | | |
| Visceral | 17 | 262 | 15 |
| Non-visceral mechanical | 29 | 526 | 18 |
| <i>Sample sex</i> | | | |
| All female | 22 | 338 | 15 |
| All male | 30 | 533 | 18 |

Table 2

Peaks of convergence of activation for meta-analyses related to acute nociceptive pain.

| Voxels | X | Y | Z | Macroanatomical Label | Cytoarchitectonic Label | Z-score |
|--------|-----|-----|-----|-----------------------|-------------------------|---------|
| 14522 | 58 | -24 | 22 | R Supramarginal Gyrus | Area PFop (IPL) | 8.52 |
| 3181 | 6 | 12 | 38 | R MCC | | 8.48 |
| 325 | -32 | -56 | -34 | L Cerebellum | Lobule VI (Hem) | 5.39 |
| 238 | 48 | 4 | 42 | R Precentral Gyrus | | 5.03 |

Note. Cluster coordinates are reported in MNI stereotaxic space. Macroanatomical labels used the SPM Anatomy Toolbox and Harvard-Oxford Structural Atlas (MCC = midcingulate cortex). Cytoarchitectonic labels were made using the SPM Anatomy Toolbox (IPL = inferior parietal lobe).

Peaks of convergence of activation for meta-analyses related to acute nociceptive pain experiments using “pain > rest” contrast and “pain > innocuous” contrast.

Table 3

| Effect of Interest | Voxels | X | Y | Z | Macroanatomical Label | Cytoarchitectonic Label | Z-score |
|-------------------------------|--------|-----|-----|-----|----------------------------|-------------------------|---------|
| Main effect: Pain > rest | | | | | | | |
| | 6936 | 58 | -24 | 22 | R Supramarginal Gyrus | Area PFOp (IPL) | 8.43 |
| | 4641 | -34 | 18 | 4 | L Insula Lobe | | 8.39 |
| | 2556 | 6 | 12 | 38 | R MCC | | 8.37 |
| | 439 | -10 | -14 | 2 | L Thalamus | Thal: Prefrontal | 8.35 |
| | 164 | -46 | -40 | 44 | L Inferior Parietal Lobule | Area hIP2 (IPS) | 4.71 |
| | 135 | -30 | -56 | -32 | L Cerebellum (VI) | Lobule VI (Hem) | 4.57 |
| | 134 | 48 | 4 | 38 | R Precentral Gyrus | | 4.59 |
| Main effect: Pain > innocuous | | | | | | | |
| | 2301 | 38 | 8 | 6 | R Insula Lobe | | 8.28 |
| | 2287 | -38 | -18 | 14 | L Insula Lobe | Area Ig2 | 7.46 |
| | 1521 | 6 | 10 | 38 | R MCC | | 7.58 |
| | 1005 | 10 | -12 | 4 | R Thalamus | Thal: Prefrontal | 6.88 |

Note. Cluster coordinates are reported in MNI stereotaxic space. Macroanatomical labels used the SPM Anatomy Toolbox and Harvard-Oxford Structural Atlas (MCC = midcingulate cortex). Cytoarchitectonic labels were made using the SPM Anatomy Toolbox (IPL = inferior parietal lobe; Thal = thalamus).

Table 4

Peaks of convergence of activation for meta-analyses related to acute thermal and non-thermal nociceptive pain.

| Effect of Interest | Voxels | X | Y | Z | Macroanatomical Label | Cytoarchitectonic Label | Z-score |
|--------------------------|--------|-----|-----|-----|------------------------|-------------------------|---------|
| Main effect: Thermal | | | | | | | |
| | 9080 | 56 | -24 | 22 | R Rolandic Operculum | Area PFop (IPL) | 8.4 |
| | 2161 | 4 | 12 | 38 | R MCC | | 8.36 |
| | 571 | 44 | 44 | 6 | R Middle Frontal Gyrus | | 7.81 |
| | 223 | -32 | -54 | -34 | L Cerebellum (VI) | Lobule VI (Hem) | 5.2 |
| | 152 | 48 | 6 | 36 | R Precentral Gyrus | | 5.32 |
| Main effect: Non-thermal | | | | | | | |
| | 4398 | 54 | 4 | 4 | R Rolandic Operculum | | 8.31 |
| | 3874 | -56 | -20 | 18 | L Postcentral Gyrus | Area OP1 [SII] | 8.31 |
| | 2094 | 8 | 12 | 36 | R MCC | | 7.53 |
| | 939 | 14 | -14 | 4 | R Thalamus | Thal: Prefrontal | 8.32 |
| | 136 | 42 | 48 | 14 | R Middle Frontal Gyrus | | 3.91 |
| Thermal > non-thermal | | | | | | | |
| | 55 | 2 | 6 | 40 | R MCC | | 8.13 |
| Non-thermal > thermal | | | | | | | |
| | 46 | 44 | 0 | -4 | R Insula Lobe | | 3.67 |
| | 40 | -40 | -32 | 20 | L Rolandic Operculum | | 3.86 |
| Thermal AND non-thermal | | | | | | | |
| | 2904 | 60 | -24 | 22 | R Supramarginal Gyrus | Area OP1 [SII] | 8.29 |
| | 2674 | -58 | -22 | 18 | L Supramarginal Gyrus | Area OP1 [SII] | 8.3 |
| | 1506 | 8 | 12 | 36 | R MCC | | 7.53 |
| | 327 | 14 | -12 | 8 | R Thalamus | Thal: Prefrontal | 7.78 |
| | 263 | -10 | -14 | 2 | L Thalamus | Thal: Prefrontal | 7.81 |
| | 127 | 42 | 48 | 14 | R Middle Frontal Gyrus | | 3.91 |

Note. Cluster coordinates are reported in MNI stereotaxic space. Macroanatomical labels were made using the SPM Anatomy Toolbox and Harvard-Oxford Structural Atlas (MCC = midcingulate cortex). Cytoarchitectonic labels were made using the SPM Anatomy Toolbox only (IPL = inferior parietal lobe; Thal = thalamus).

Table 5
Peaks of convergence of activation for meta-analyses related to acute electrical and mechanical nociceptive pain.

| Effect of Interest | Voxels | X | Y | Z | Macroanatomical Label | Cytoarchitectonic Label | Z-score |
|-----------------------------------|--------|-----|-----|-----|---------------------------|-------------------------|---------|
| Main effect: Electrical | | | | | | | |
| | 1901 | 54 | 2 | 6 | R Rolandic Operculum | | 7.52 |
| | 1514 | -56 | -20 | 20 | L Postcentral Gyrus | Area OP1 [SII] | 6.17 |
| | 729 | 10 | 12 | 38 | R MCC | | 4.87 |
| | 249 | 14 | -16 | 6 | R Thalamus | Thal: Prefrontal | 6.59 |
| | 202 | -12 | -16 | 8 | L Thalamus | Thal: Prefrontal | 5.27 |
| Main effect: mechanical | | | | | | | |
| | 1354 | 34 | 6 | 8 | R Insula Lobe | | 5.63 |
| | 848 | -44 | 0 | 6 | L Insula Lobe | | 5.19 |
| | 814 | -54 | -22 | 16 | L Supramarginal Gyrus | Area OP1 [SII] | 7.39 |
| | 755 | 58 | -26 | 24 | R Supramarginal Gyrus | Area PPop (IPL) | 7.46 |
| | 501 | 4 | 14 | 34 | R MCC | | 5.7 |
| | 227 | -12 | -14 | 4 | L Thalamus | Thal: Prefrontal | 6.76 |
| | 164 | 12 | -12 | 2 | R Thalamus | Thal: Prefrontal | 6.9 |
| Electrical > mechanical | | | | | | | |
| | 33 | 44 | -20 | 22 | R Rolandic Operculum | | 3.83 |
| | 26 | 6 | -18 | 10 | R Thalamus | Thal: Temporal | 3.54 |
| | 25 | 46 | 2 | -16 | R Superior Temporal Gyrus | | 3.45 |
| Mechanical > electrical | | | | | | | |
| <i>No suprathreshold clusters</i> | | | | | | | |
| Electrical AND mechanical | | | | | | | |
| | 466 | 36 | 6 | 10 | R Insula Lobe | | 4.76 |
| | 462 | -56 | -20 | 18 | L Postcentral Gyrus | Area OP1 [SII] | 6.06 |
| | 334 | 60 | -22 | 20 | R Supramarginal Gyrus | Area OP1 [SII] | 5.47 |
| | 275 | -36 | 4 | 12 | L Insula Lobe | | 5.05 |
| | 243 | 8 | 14 | 36 | R MCC | | 4.62 |
| | 113 | -14 | -16 | 8 | L Thalamus | Thal: Prefrontal | 5.01 |
| | 98 | 14 | -14 | 6 | R Thalamus | Thal: Prefrontal | 5.8 |

Note: Cluster coordinates are reported in MNI stereotaxic space. Macroanatomical labels were made using the SPM Anatomy Toolbox and Harvard-Oxford Structural Atlas (MCC = midcingulate cortex). Cytoarchitectonic labels were made using the SPM Anatomy Toolbox only (Thal = thalamus).

Author Manuscript

Author Manuscript

Author Manuscript

Author Manuscript

Table 6

Peaks of convergence of activation for meta-analyses related to acute nociceptive chemical pain.

| Voxels | X | Y | Z | Macroanatomical Label | Cytoarchitectonic Label | Z-score |
|--------|-----|-----|-----|-----------------------|-------------------------|---------|
| 663 | 38 | 16 | -6 | R Insula Lobe | | 5.29 |
| 534 | -58 | -4 | 8 | L Rolandic Operculum | Area OP4 [PV] | 4.78 |
| 449 | 62 | -14 | 20 | R Postcentral Gyrus | Area PFop (IPL) | 4.43 |
| 329 | -10 | 12 | 38 | L MCC | | 5.22 |
| 232 | -34 | 10 | 2 | L Insula Lobe | | 5.26 |
| 183 | -2 | -2 | 62 | L SMA | | 4.85 |
| 163 | 14 | -14 | 6 | R Thalamus | Thal: Prefrontal | 5.35 |
| 154 | -12 | -20 | -4 | L Thalamus | Thal: Motor | 5.19 |
| 117 | -6 | -40 | -50 | Brainstem | | 5.19 |
| 105 | -36 | -8 | 4 | L Insula Lobe | | 4.1 |

Note. Cluster coordinates are reported in MNI stereotaxic space. Macroanatomical labels were made using the SPM Anatomy Toolbox and Harvard-Oxford Structural Atlas (SMA = supplementary motor area). Cytoarchitectonic labels were made using the SPM Anatomy Toolbox (IPL = inferior parietal lobe; Thal = thalamus).

Table 7
Peaks of convergence of activation for meta-analyses related to left-sided and right-sided acute nociceptive pain.

| Effect of Interest | Voxels | X | Y | Z | Macroanatomical Label | Cytoarchitectonic Label | Z-score |
|--------------------|-----------------------------------|-----|-----|-----|----------------------------|-------------------------|---------|
| Main effect: Left | | | | | | | |
| | 5034 | 40 | -16 | 16 | R Rolandic Operculum | Area OP3 [VS] | 8.34 |
| | 3096 | -60 | -24 | 20 | L Supramarginal Gyrus | Area PFop (IPL) | 8.31 |
| | 1445 | 6 | 12 | 38 | R MCC | | 8.29 |
| | 236 | 44 | 44 | 6 | R Middle Frontal Gyrus | | 5.73 |
| | 137 | -32 | -56 | -32 | L Cerebellum (VI) | Lobule VI (Hem) | 4.62 |
| | 125 | 24 | -44 | 68 | R Postcentral Gyrus | Area I | 5.87 |
| Main effect: Right | | | | | | | |
| | 2944 | -40 | -18 | 14 | L Rolandic Operculum | Area Ig2 | 8.27 |
| | 1743 | 38 | 20 | 4 | R Insula Lobe | | 7.61 |
| | 1737 | 6 | 12 | 38 | R MCC | | 7.63 |
| | 689 | 58 | -22 | 22 | R Supramarginal Gyrus | Area PFop (IPL) | 8.28 |
| | 301 | 44 | 44 | 6 | R Middle Frontal Gyrus | | 5.99 |
| | 224 | -12 | -14 | 4 | L Thalamus | Thal: Prefrontal | 6.16 |
| | 217 | 50 | 2 | 44 | R Precentral Gyrus | | 5.31 |
| | 170 | 14 | -14 | 6 | R Thalamus | Thal: Prefrontal | 5.06 |
| | 143 | 52 | -38 | 46 | R Inferior Parietal Lobule | Area PFm (IPL) | 4.1 |
| Left > right | <i>No suprathreshold clusters</i> | | | | | | |
| Right > left | 45 | -44 | -22 | 16 | L Rolandic Operculum | Area OPI [SII] | 6.8 |
| Left AND right | 1437 | -32 | 18 | 6 | L Insula Lobe | | 7.11 |
| | 1318 | 38 | 20 | 0 | R Insula Lobe | | 6.76 |
| | 1116 | 6 | 12 | 38 | R MCC | | 7.63 |
| | 608 | 58 | -22 | 22 | R Supramarginal Gyrus | Area PFop (IPL) | 8.28 |
| | 542 | -58 | -26 | 20 | L Supramarginal Gyrus | Area PFop (IPL) | 8.08 |
| | 178 | 44 | 44 | 6 | R Middle Frontal Gyrus | | 5.73 |

| Effect of Interest | Voxels | X | Y | Z | Macroanatomical Label | Cytoarchitectonic Label | Z-score |
|--------------------|--------|-----|-----|---|-----------------------|-------------------------|---------|
| | 167 | 14 | -14 | 6 | R Thalamus | Thal: Prefrontal | 5.06 |
| | 158 | -12 | -14 | 4 | L Thalamus | Thal: Prefrontal | 6.16 |

Note. Cluster coordinates are reported in MNI stereotaxic space. Macroanatomical labels were made using the SPM Anatomy Toolbox and Harvard-Oxford Structural Atlas (MCC = midcingulate cortex). Cytoarchitectonic labels were made using the SPM Anatomy Toolbox only (IPL = inferior parietal lobe; Thal = thalamus; VS = ventral somatosensory).

Table 8

Peaks of convergence of activation for meta-analyses related to distal and proximal acute nociceptive pain.

| Effect of Interest | Voxels | X | Y | Z | Macroanatomical Label | Cytoarchitectonic Label | Z-score |
|-----------------------------------|--------|-----|-----|----|------------------------|-------------------------|---------|
| Main effect: Distal | | | | | | | |
| | 3044 | 56 | -26 | 22 | R Rolandic Operculum | Area PFop (IPL) | 8.3 |
| | 2579 | -60 | -24 | 20 | L Supramarginal Gyrus | Area PFop (IPL) | 8.28 |
| | 1384 | 4 | 10 | 38 | R MCC | | 6.46 |
| | 605 | 12 | -12 | 4 | R Thalamus | Thal: Prefrontal | 6.68 |
| | 222 | 46 | 42 | 6 | R Middle Frontal Gyrus | | 4.72 |
| | 162 | -10 | -12 | 2 | L Thalamus | Thal: Prefrontal | 6.21 |
| Main effect: Proximal | | | | | | | |
| | 4319 | 38 | -18 | 16 | R Rolandic Operculum | Area OP2 [PIVC] | 8.32 |
| | 3261 | -36 | 4 | 8 | L Insula Lobe | | 8.31 |
| | 1696 | 6 | 12 | 38 | R MCC | | 8.31 |
| | 227 | 44 | 44 | 6 | R Middle Frontal Gyrus | | 6.05 |
| | 223 | 48 | 6 | 38 | R Precentral Gyrus | | 5.62 |
| | 182 | 22 | -44 | 68 | R Postcentral Gyrus | Area 1 | 6.5 |
| Distal > proximal | | | | | | | |
| <i>No suprathreshold clusters</i> | | | | | | | |
| Proximal > distal | | | | | | | |
| <i>No suprathreshold clusters</i> | | | | | | | |
| Distal AND proximal | | | | | | | |
| | 2041 | 56 | -24 | 22 | R Rolandic Operculum | Area PFop (IPL) | 8.3 |
| | 1156 | -34 | 20 | 4 | L Insula Lobe | | 7.25 |
| | 917 | 4 | 10 | 38 | R MCC | | 6.46 |
| | 854 | -60 | -24 | 20 | L Supramarginal Gyrus | Area PFop (IPL) | 8.28 |
| | 258 | 12 | -12 | 4 | R Thalamus | Thal: Prefrontal | 6.68 |
| | 153 | -10 | -12 | 2 | L Thalamus | Thal: Prefrontal | 6.21 |
| | 97 | 46 | 42 | 6 | R Middle Frontal Gyrus | | 4.69 |
| | 77 | 16 | 4 | 0 | R Pallidum | | 4.01 |

Note. Cluster coordinates are reported in MNI stereotaxic space. Macroanatomical labels were made using the SPM Anatomy Toolbox and Harvard-Oxford Structural Atlas (MCC = midcingulate cortex). Cytoarchitectonic labels were made using the SPM Anatomy Toolbox only (IPL = inferior parietal lobe; Thal = thalamus).

Table 9
Peaks of convergence of activation for meta-analyses related to acute visceral and non-visceral nociceptive pain.

| Effect of Interest | Voxels | X | Y | Z | Macroanatomical Label | Cytoarchitectonic Label | Z-score |
|--------------------------------------|--------|-----|-----|----|-----------------------|-------------------------|---------|
| Main effect: Visceral | | | | | | | |
| | 431 | 60 | -24 | 26 | R Supramarginal Gyrus | Area PFop (IPL) | 6.14 |
| | 237 | -32 | 0 | -2 | L Putamen | | 4.76 |
| | 174 | 54 | -6 | 8 | R Rolandic Operculum | Area OP4 [PV] | 4.66 |
| | 142 | -8 | -14 | -2 | L Thalamus | Thal: Prefrontal | 4.89 |
| | 91 | 8 | 16 | 36 | R MCC | | 4.2 |
| Main effect: Non-visceral mechanical | | | | | | | |
| | 606 | -56 | -24 | 18 | L Supramarginal Gyrus | Area OPI [SII] | 5.93 |
| | 394 | -44 | 2 | 4 | L Insula Lobe | | 5.24 |
| | 351 | 60 | -22 | 18 | R Supramarginal Gyrus | Area OPI [SII] | 5.71 |
| | 272 | 4 | 14 | 34 | R MCC | | 4.71 |
| | 185 | 44 | 18 | 0 | R Insula Lobe | | 4.59 |
| | 150 | 54 | 8 | 6 | R Rolandic Operculum | Area 44 | 4.31 |
| | 140 | 36 | 6 | 6 | R Insula Lobe | | 4.87 |
| | 128 | 20 | 14 | 4 | R Caudate | | 4.38 |
| | 108 | -14 | -14 | 4 | L Thalamus | Thal: Prefrontal | 5.52 |
| | 100 | 14 | -12 | 4 | R Thalamus | Thal: Prefrontal | 5 |
| Visceral > Non-visceral mechanical | | | | | | | |
| Non-visceral mechanical > visceral | | | | | | | |
| Visceral AND Non-visceral mechanical | | | | | | | |
| | 136 | 58 | -28 | 24 | R Supramarginal Gyrus | Area PFcm (IPL) | 5.18 |
| | 74 | -10 | -14 | 2 | L Thalamus | Thal: Prefrontal | 4.49 |

Note. Cluster coordinates are reported in MNI stereotaxic space. Macroanatomical labels were made using the SPM Anatomy Toolbox and Harvard-Oxford Structural Atlas (MCC = midcingulate cortex). Cytoarchitectonic labels were made using the SPM Anatomy Toolbox only (IPL = inferior parietal lobe; Thal = thalamus).

Table 10

Peaks of convergence of activation for meta-analyses related to all-female and all-male samples.

| Effect of Interest | Voxels | X | Y | Z | Macroanatomical Label | Cytoarchitectonic Label | Z-score |
|---------------------|-----------------------------------|-----|-----|----|---------------------------|-------------------------|---------|
| Main effect: Female | | | | | | | |
| | 315 | -32 | 16 | 8 | L Insula Lobe | | 6.36 |
| | 249 | -64 | -28 | 22 | L Superior Temporal Gyrus | Area PFop (IPL) | 5.02 |
| | 213 | 38 | 16 | -2 | R Insula Lobe | | 4.48 |
| | 142 | -40 | -4 | 0 | L Insula Lobe | | 4.27 |
| | 98 | 62 | -20 | 24 | R Supramarginal Gyrus | Area PFI (IPL) | 4.98 |
| Main effect: Male | | | | | | | |
| | 1115 | -34 | 20 | 0 | L Insula Lobe | | 6.76 |
| | 547 | 8 | 14 | 36 | R MCC | | 6.39 |
| | 477 | 36 | 22 | 2 | R Insula Lobe | | 6.52 |
| | 374 | 56 | 12 | -4 | R Temporal Pole | Area TE 3 | 5.03 |
| | 305 | 56 | -26 | 22 | R Rolandic Operculum | Area PFop (IPL) | 4.87 |
| | 274 | 44 | 46 | 4 | R Middle Frontal Gyrus | | 6.05 |
| | 189 | -10 | -12 | 4 | L Thalamus | Thal: Prefrontal | 5.98 |
| | 169 | 14 | -14 | 8 | R Thalamus | Thal: Prefrontal | 5.59 |
| Female > male | <i>No suprathreshold clusters</i> | | | | | | |
| Male > female | <i>No suprathreshold clusters</i> | | | | | | |
| Female AND male | | | | | | | |
| | 141 | -62 | -26 | 22 | L Supramarginal Gyrus | Area PFop (IPL) | 4.88 |
| | 88 | -32 | 18 | 4 | L Insula Lobe | | 5.13 |
| | 58 | 38 | 18 | -2 | R Insula Lobe | | 4.14 |

Note. Cluster coordinates are reported in MNI stereotaxic space. Macroanatomical labels were made using the SPM Anatomy Toolbox and Harvard-Oxford Structural Atlas (MCC = midcingulate cortex). Cytoarchitectonic labels were made using the SPM Anatomy Toolbox only (IPL = inferior parietal lobe; Thal = thalamus).